J. Fluid Mech. (2013), *vol.* 719, *pp.* 129–164. © Cambridge University Press 2013
doi:10.1017/jfm.2012.635

Multimodal analysis of weakly nonlinear sloshing in a spherical tank

Odd M. Faltinsen† and Alexander N. Timokha

Centre for Ships and Ocean Structures and Department of Marine Technology, Centre for Autonomous Marine Operations and Systems, Norwegian University of Science and Technology, NO-7091, Trondheim, Norway

(Received 17 August 2012; revised 26 October 2012; accepted 16 December 2012; first published online 19 February 2013)

Sloshing in a spherical tank due to horizontal excitation is studied by using the nonlinear multimodal method which involves the analytically approximate sloshing modes by Faltinsen & Timokha (*J. Fluid Mech.*, vol. 703, 2012, pp. 391–401). General fully and weakly nonlinear modal equations are derived but an emphasis is on the Moiseev–Narimanov asymptotic modal system which implies that the forcing frequency is close to the lowest natural sloshing frequency and there are no secondary resonances in the forcing frequency range leading to a nonlinear resonant amplification of double and triple harmonics in higher modes. The Moiseev–Narimanov modal system is used to construct an asymptotic time-periodic solution and, thereby, classify the corresponding steady-state wave regimes appearing as stable and unstable planar waves and swirling. The results on the stability boundaries are compared with experiments by Sumner & Stofan (1963, *Tech. Rep.* TN D-1991, NASA Technical Note) and Sumner (1966, *Tech. Rep.* TN D-3210, NASA). A good agreement is established for $0.2 \leqslant h \lesssim 1$. Discrepancy for higher liquid depths $1 \lesssim h < 2$ are explained by secondary resonance.

Key words: interfacial flows (free surface)

1. Introduction

Spherical tanks are used, for instance, on ships for liquefied natural gas (LNG) transportation. Resonant sloshing in partially filled LNG tanks with the forcing frequency in the vicinity of the lowest natural sloshing frequency is of particular concern. Because the lateral tank excitation amplitude can be as high as of the order of 10 % of the tank diameter, the free-surface nonlinearity plays a significant role and, as a consequence, there occur strongly nonlinear three-dimensional wave motions, e.g. steady-state rotary wave motions (swirling) with resulting large hydrodynamic force in both the excitation direction and perpendicular to the excitation direction in the horizontal plane. Furthermore, the stable steady-state wave motions may not exist in certain frequency ranges dependent on the filling level and the excitation amplitude. The majority of theoretical publications is restricted to linear theory associated with non-resonant excitation and small forcing magnitude. Examples are

† Email address for correspondence: oddfal@marin.ntnu.no

https://doi.org/10.1017/jfm.2012.635 Published online by Cambridge University Press

given by Budiansky (1958, 1960), McIver (1989), Karamanos, Papaprokopiou & Platyrrachos (2006, 2009), Patkas & Karamanos (2007), Drodos, Dimas & Karabalis (2008), Hasheminejad & Aghabeigi (2009) and Utsumi (2011).

The subject of liquid sloshing needs a combination of analytical methods, computational fluid dynamics (CFD) and model tests. To the best of the authors' knowledge, the present paper makes the first step towards creating a semi-analytical theory of nonlinear resonant liquid sloshing in a spherical tank. Bearing in mind unique weakly nonlinear semi-analytical theories for the circle- and square-base upright tanks by Miles (1984*a*,*b*), Gavrilyuk, Lukovsky & Timokha (2000), Faltinsen, Rognebakke & Timokha (2003) and Gavrilyuk *et al.* (2007), the multimodal method is employed. Within the assumptions that an inviscid incompressible liquid is in irrotational flow, the liquid surface does not overturn or break, and the surface tension does not matter, the multimodal method can provide accurate measures of the physically important sloshing-induced hydrodynamic forces and moments on the vessel. However, its main mission is to facilitate systematic parameter studies including the study of resonant three-dimensional sloshing regimes and their stability, the so-called theoretical classification (Faltinsen, Rognebakke & Timokha 2005*a*). From a computational point of view, the classification suggests analysing how the three-dimensional forced sloshing changes on the long-time scale versus a broad set of input parameter and diverse initial scenarios. Traditional CFD requires a huge computational time to solve this task. In the current literature, the modal methods, in general, and the multimodal method, in particular, have no alternative for conducting the classification. This was already done for upright circular cylindrical (Miles 1984*a*,*b*), square-base (Faltinsen *et al.* 2003, 2005*a*) and V-conical (Gavrilyuk, Lukovsky & Timokha 2005) tanks, but not for the spherical tank shape. When analysing the experimental resonant sloshing regimes in a spherical tank, Sumner & Stofan (1963) and Sumner (1966) assigned them with those occurring for a spherical pendulum which were later on found to be qualitatively the same as for resonant sloshing in an upright circular cylindrical tank with a finite liquid depth (see discussions by Miles (1962, 1976, 1984*a*,*b*)). Our goal is to get, in the manner of Faltinsen *et al.* (2003, 2005*a*), the theoretical classification of the nonlinear resonant steady-state wave regimes in a spherical tank due to horizontal harmonic tank excitation.

The multimodal method derives a system of nonlinear ordinary differential equations coupling the generalized coordinates responsible for the free-surface motion in terms of the natural sloshing modes. The derivation procedure is well elaborated for upright circular cylindrical tanks (Lukovsky 1990; Gavrilyuk *et al.* 2000; Lukovsky, Ovchynnykov & Timokha 2012; Takahara & Kimura 2012) and square-base tanks (Faltinsen *et al.* 2003; Faltinsen, Firoozkoohi & Timokha 2011) when there exist exact analytical sloshing modes and a single-valued representation of the free surface *a priori* satisfying the volume conservation condition. Even though the procedure could look analytically tedious, dealing with huge analytical expressions, the multimodal method has become increasingly popular among applied mathematicians and engineers (see, e.g., Love & Tait 2010, 2011; Ansari, Firouz-Abadi & Ghasemi 2011; Antuono *et al.* 2012; Ikeda *et al.* 2012; Takahara & Kimura 2012; Takahara, Hara & Ishida 2012) whose interests are parameter studies of nonlinear sloshing problems.

Generalizing the multimodal method to complex tank shapes with non-cylindrical walls at the free surface requires two tasks to be solved. The first task consists of getting a single-valued representation of the free surface which becomes

https://doi.org/10.1017/jfm.2012.635 Published online by Cambridge University Press

possible, e.g., in appropriate curvilinear coordinate systems (transformation of spatial coordinates was called the non-conformal mapping technique by Lukovsky (1975)). The second task is specific requirements to the corresponding approximate natural sloshing modes which must be analytically given harmonic functions exactly satisfying the body-boundary condition and being analytically expandable over the mean free surface. Generalizing the nonlinear multimodal method to the V-shaped conical tank became possible due to approximate analytical modes by Lukovsky & Timokha (2002) and Gavrilyuk *et al.* (2005, 2008). Barnyak *et al.* (2011) and Faltinsen & Timokha (2012) constructed appropriate analytically approximate modes for a spherical tank which are a background of the present paper.

The paper presents three nonlinear modal systems. In §§ 2 and 3, we derive the fully nonlinear modal equations which couple generalized coordinates and velocities and generalize the fully nonlinear modal equations in chap. 7 by Faltinsen & Timokha (2009) derived for upright cylindrical tanks. The modal equations include two subsystems implying kinematic and dynamic relations, respectively, and can facilitate direct time simulations of nonlinear transient waves using the method of Perko (Moore & Perko 1964; Perko 1969; La Rocca, Scortino & Boniforti 2000). To investigate differences caused by the tank geometry, we follow the scheme by Faltinsen *et al.* (2003) to derive a weakly-nonlinear modal system (§ 3.4) with respect to the generalized coordinates. For this purpose, the kinematic subsystem from § 3 is asymptotically resolved in a neighbourhood of zero to find the generalized velocities as functions of the generalized coordinates and their derivatives. Such a weakly nonlinear infinite-dimensional system of modal equations is known for rectangular tanks (Zakharov 1968; Faltinsen & Timokha 2001; Faltinsen *et al.* 2003; Love & Tait 2010, 2011) but it is a novelty for non-cylindrical tank shapes. Employing the weakly nonlinear modal system makes it possible to derive different asymptotic modal equations including those based on Moiseev–Narimanov's and adaptive asymptotics. We concentrate on nonlinear modal equations following from the Moiseev–Narimanov asymptotics which is typical for nonlinear sloshing in tanks with finite liquid depth. The asymptotics was mathematically justified by Narimanov (1957) and Moiseev (1958) who showed that, when a rigid tank is forced with a small horizontal excitation magnitude characterized by a non-dimensional parameter $\epsilon \ll 1$ and the (mean) forcing frequency σ is close to the lowest natural sloshing frequency, the resonant wave response has the order $O(\epsilon^{1/3})$. When the tank is axisymmetric, the dominant $O(\epsilon^{1/3})$ contribution is associated with the two lowest perpendicular natural sloshing modes characterized by the same lowest natural sloshing frequency. Adopting the Moiseev–Narimanov result yields special third-order asymptotic intermodal relations between generalized coordinates and velocities in the nonlinear modal equations. Using these relations helps us to derive a compact system of nonlinear modal equations which could be a base for analytical studies on resonant liquid sloshing. For three-dimensional rectangular tanks, this leads to a finite-dimensional modal system but axisymmetric tanks cause an infinite-dimensional modal system exemplified by Lukovsky *et al.* (2012) and Takahara & Kimura (2012) for upright circular (annular) cylindrical tanks. In § 4.2, we derive the Moiseev–Narimanov modal system for a spherical tank. A necessary condition for the Moiseev–Narimanov asymptotics to be valid is no secondary resonances causing higher modes to be amplified up to the dominant asymptotic order. Furthermore, there are no other small non-dimensional parameters, e.g. a shallow liquid depth.

https://doi.org/10.1017/jfm.2012.635 Published online by Cambridge University Press

Damping terms can be incorporated into the derived nonlinear modal equations as it is extensively discussed in chapters 8 and 9 of Faltinsen & Timokha (2009) (see also references therein and extensive discussions in Faltinsen, Rognebakke & Timokha (2005*b*, 2006) and Faltinsen *et al.* (2011)). The viscous damping due to the boundary layer flow for a clean tank is more important than the damping due to the bulk viscosity. If the boundary layer is laminar as is typically the case in model test conditions, the associated damping can be estimated within the framework of linear theory. However, the latter damping for realistic liquid cargoes is very small relative to the critical damping. The boundary layer damping ratios have the order of the experimental non-dimensional forcing amplitude ϵ in model tests by Sumner & Stofan (1963) observing nonlinear liquid sloshing and, therefore, neglecting the $O(\epsilon)$-order terms implies asymptotically negligible influence of the boundary-layer damping (for more details see § 4.2). The amount of dissipation increases when wave breaking and overturning occur but there is no a well-established strategy how to account for it in the multimodal methods.

Assuming small-amplitude harmonic horizontal tank excitations, the derived Moiseev–Narimanov system is used in § 4.3 for getting an asymptotic steady-state (time-periodic) solution and studying its stability. The solution identifies planar waves and swirling. A region where stable steady-state wave regimes do not exist implies irregular waves. These three types of wave motions were described in the experimental NASA reports by Sumner & Stofan (1963) and Sumner (1966) who also evaluated the stability boundaries between them. An emphasis in the present investigation is on theoretical stability boundaries and their validation by comparison with these experiments, i.e. on the so-called theoretical classification of the resonant steady-state wave regimes. A good agreement is found for the liquid depth-to-radius ratios $0.2 < h \lesssim 1$. However, applicability of the Moiseev–Narimanov modal theory is limited for higher liquid depths due to secondary resonances and near-wall overturning waves ('splashing') described by Sumner & Stofan (1963) as 'drops splashed from the tank wall and showered through the ullage'. A clarification of 'splashing' to occur needs a new theoretical concept, but a theoretical estimate of the secondary resonance is done in § 4.3 within the framework of the constructed asymptotic (time-periodic) solution. According to our analysis, occurrence of secondary resonances is unavoidable at the four critical liquid depth-to-radius ratios $h = h_{Mi} : h_{02} = 1.219\ldots, h_{22} = 1.129\ldots, h_{32} = 1.529\ldots$ and $h_{13} = 1.642\ldots$ causing the corresponding natural sloshing modes to give a dominant contribution through amplification of double/triple forcing harmonics. The Moiseev–Narimanov modal theory is invalid for these depths. Furthermore, even though the non-dimensional liquid depths $h = 1.4$ and 1.8 are not critical, experiments by Sumner & Stofan (1963) show that the secondary resonance phenomenon (and near-wall overturning waves) matter for these depths. Further modifications to extend the multimodal method for description of the secondary resonance are discussed in § 5.

2. Variational formulation and general modal equations

2.1. *Bateman–Luke variational formulation*

We consider sloshing in a spherical tank of radius R_0 occurring due to a translatory horizontal oscillatory motions whose magnitude is small relative to the tank radius R_0. The analysis will be done with a non-dimensional statement which suggests the characteristic dimension R_0 and the characteristic time $\sqrt{R_0/g}$ where g is the gravity acceleration. As a consequence, the theoretical tank has unit radius and the horizontal

https://doi.org/10.1017/jfm.2012.635 Published online by Cambridge University Press

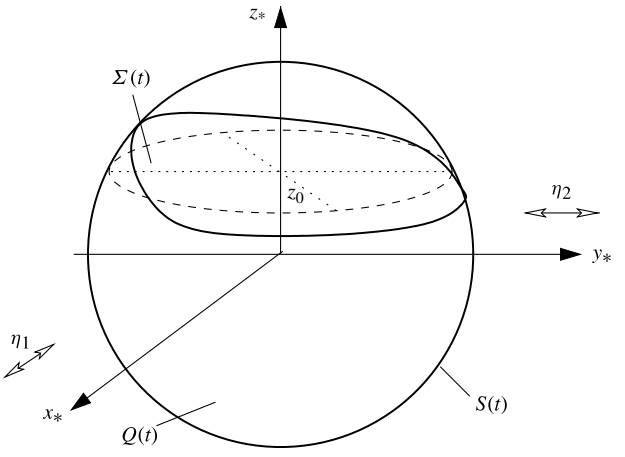


FIGURE 1. Sketch of a spherical tank partly filled by a liquid in the physical space $Ox_*y_*z_*$. Also shown are the instantaneous liquid volume $Q(t)$, the free surface $\Sigma(t)$ and the wetted tank surface $S(t)$. The tank performs small-magnitude horizontal oscillatory motions governed by $\eta_1(t)$ and $\eta_2(t)$.

tank displacements $(\eta_1(t), \eta_2(t), 0)$ in figure 1 are assumed to be non-dimensional (scaled by R_0).

The liquid is ideal and incompressible with irrotational flows. The surface tension is neglected. The corresponding non-dimensional free-surface problem is normally formulated in the tank-fixed (non-inertial) coordinate system $Ox_*y_*z_*$ with the origin in the sphere centre so that the free surface $\Sigma(t)$ is implicitly defined by the equation $Z = Z(x_*, y_*, z_*, t) = 0$. The non-dimensional velocity potential $\Phi(x_*, y_*, z_*, t)$ describes the absolute liquid velocity, i.e. $\nabla \cdot \Phi$ is the liquid velocity considered in an absolute (inertial) coordinate system. Details can be found in § 2.4.2 of Faltinsen & Timokha (2009). Here, Φ and Z are the unknowns.

Instead of dealing with the corresponding free-boundary problem, we will employ the Bateman–Luke variational formulation which was originated by Hargneaves (1908), Bateman (1944) and Luke (1967) for the external surface-wave problems. Equivalence to the original differential sloshing problem in which the free surface $\Sigma(t)$ is implicitly defined is proved in chap. 2 of Lukovsky & Timokha (1995) and § 2.5.3.2 of Faltinsen & Timokha (2009). According to this variational formulation, the solution (Φ and the liquid volume evolution $Q(t)$ defined by $Z = 0$) coincides with the extrema points of the action

$$\mathscr{A}(Z, \Phi) = \int_{t_1}^{t_2} \int_{Q(t)} \left[\frac{\partial \Phi}{\partial t} + \frac{1}{2} (\nabla_* \Phi)^2 - \frac{\partial \Phi}{\partial x_*} \dot{\eta}_1 - \frac{\partial \Phi}{\partial y_*} \dot{\eta}_2 + z_* \right] \mathrm{d}x_* \, \mathrm{d}y_* \, \mathrm{d}z_* \, \mathrm{d}t \quad (2.1)$$

for arbitrary instant times t_1 and t_2 ($t_1 < t_2$) subject to independent variations of Φ and Z satisfying

$$\delta \Phi|_{t_1, t_2} = 0, \quad \delta Z|_{t_1, t_2} = 0. \quad (2.2)$$

2.2. *General modal equations*

The Bateman–Luke formulation was used in chap. 9 of Faltinsen & Timokha (2009) for derivations of fully nonlinear modal equations when the tank has vertical walls

https://doi.org/10.1017/jfm.2012.635 Published online by Cambridge University Press

at the mean free surface and the single-valued representation of the free surface $\Sigma(t): Z = z_* - f(x_*, y_*, t) = 0$ is possible in the Cartesian coordinate system $Ox_*y_*z_*$. The function f is expanded in a Fourier series with the time-dependent coefficients $\{\beta_N(t)\}$ playing the role of generalized coordinates. Because the spherical tank surface is not cylindrical about the mean free surface in the free-surface zone, this representation is impossible for the studied case. Thus, we have to introduce the generalized coordinates implicitly, by postulating

$$Z = Z(x_*, y_*, z_*; \{\beta_N(t)\}) \tag{2.3}$$

subject to the volume conservation condition

$$\text{const} = V_l = \int_{Q(t)} \mathrm{d}x_*\,\mathrm{d}y_*\,\mathrm{d}z_* = \pi\left[\frac{2}{3} + z_0\left(1 - \frac{1}{3}z_0^2\right)\right] \tag{2.4}$$

which can be associated with a holonomic constraint coupling $\{\beta_N(t)\}$. Here, $z_0 = h - 1$ is defined, e.g., in figure 1.

Furthermore, we introduce the modal solution for the velocity potential

$$\Phi(x_*, y_*, z_*, t) = \dot\eta_1(t)x_* + \dot\eta_2(t)y_* + \sum_N F_N(t)\varphi_N(x_*, y_*, z_*), \tag{2.5}$$

which is a generalization of the exact linear modal solution (see, chap. 5 by Faltinsen & Timokha 2009). Here $\{\varphi_N\}$ is a complete set of linearly independent harmonic functions defined in $Q(t)$ for any admissible instant liquid shapes and $\{F_N(t)\}$ play the role of generalized velocities. Even though $\{\varphi_N\}$ does not need to be the natural sloshing modes (eigensolution of the corresponding spectral boundary problem), practical realizations of the multimodal method are typically based on the natural sloshing modes. The Fourier-type harmonic solution (2.5) should exactly satisfy the Neumann boundary condition on the wetted tank walls in order to avoid errors due to failure in satisfying the volume (mass) conservation.

Because Z and Φ in the Bateman–Luke action $\mathscr{A}$ are independent, the generalized coordinates $\{\beta_N\}$ and velocities $\{F_N\}$ are also independent and conditions $\delta F_N|_{t=t_1,t_2} = \delta\beta_N|_{t=t_1,t_2} = 0$ follow from (2.2).

After substitution of (2.3) and (2.5) into (2.1) the action becomes a function of the independent generalized coordinates $\{\beta_N(t)\}$ and velocities $\{F_N(t)\}$. By employing the standard calculus-of-variations technique, the extrema condition with respect to the generalized coordinates and velocities ($\delta\beta_N|_{t_1,t_2} = 0$ and $\delta F_N|_{t_1,t_2} = 0$ due to (2.2)) leads to a system of ordinary differential equations (modal equations) with respect to β_N and F_N. The derivation scheme is described in chap. 7 of Faltinsen & Timokha (2009). The modal equations consist of kinematic

$$\frac{\mathrm{d}A_N}{\mathrm{d}t} \equiv \sum_K \frac{\partial A_N}{\partial \beta_K}\dot\beta_K = \sum_K A_{NK}F_K \quad \text{for all } N \tag{2.6}$$

and dynamic

$$\sum_K \frac{\partial A_K}{\partial \beta_N}\dot F_K + \frac{1}{2}\sum_{KL}\frac{\partial A_{KL}}{\partial \beta_N}F_kF_L + \frac{\partial l_1}{\partial \beta_N}\ddot\eta_1 + \frac{\partial l_2}{\partial \beta_N}\ddot\eta_2 + \frac{\partial l_3}{\partial \beta_N} = 0 \quad \text{for all } N \tag{2.7}$$

https://doi.org/10.1017/jfm.2012.635 Published online by Cambridge University Press

subsystems. Because the liquid domain $Q(t)$ and the free surface $\Sigma(t)$ are determined by the equation $Z(x_*, y_*, z_*; \{\beta_N(t)\}) = 0$, we get

$$A_N = \int_{Q(t)} \varphi_N \, \mathrm{d}x_* \, \mathrm{d}y_* \, \mathrm{d}z_*; \quad A_{NK} = \int_{Q(t)} (\nabla_* \varphi_N \cdot \nabla_* \varphi_K) \, \mathrm{d}x_* \, \mathrm{d}y_* \, \mathrm{d}z_*, \tag{2.8a}$$

$$l_1 = \int_{Q(t)} x_* \, \mathrm{d}x_* \, \mathrm{d}y_* \, \mathrm{d}z_*; \quad l_2 = \int_{Q(t)} y_* \, \mathrm{d}y_* \, \mathrm{d}y_* \, \mathrm{d}z_*; \quad l_3 = \int_{Q(t)} z_* \, \mathrm{d}x_* \, \mathrm{d}y_* \, \mathrm{d}z_*. \tag{2.8b}$$

The variables A_N, A_{NK} and l_i are complicated nonlinear functions of the generalized coordinates $\{\beta_N(t)\}$.

To obtain an explicit analytical form of (2.6) and (2.7), we require an explicit expression for (2.3) and the aforementioned analytically given natural sloshing modes $\{\varphi_N\}$ which exactly satisfy the Laplace equation, the zero Neumann condition on a wetted tank surface and keep integrals (2.8) mathematically correct.

3. Modal equations (2.6) and (2.7) for a spherical tank

For the spherical tank shape, the natural sloshing modes $\{\varphi_N(t)\}$ are naturally expressed in cylindrical coordinate system whose vertical axis is perpendicular to the mean free surface and crosses its centre (see McIver (1989) and Faltinsen & Timokha (2012) and references therein). Modal equations (2.6) and (2.7) require analytically approximate natural sloshing modes $\{\varphi_N(t)\}$ which: (i) satisfy the zero Neumann condition on the mean wetted tank surface; and (ii) are expandable over the mean free surface. Furthermore, an explicit analytical representation (2.3) should be postulated.

3.1. *Modal representation of the velocity potential*

The natural sloshing modes $\{\varphi_N\}$ are eigenfunctions of the spectral boundary problem

$$\nabla^2 \varphi_N = 0 \quad \text{in } Q_0, \quad \frac{\partial \varphi_N}{\partial n} = 0 \quad \text{on } S_0, \quad \frac{\partial \varphi_N}{\partial n} = \kappa_N \varphi_N \quad \text{on } \Sigma_0, \tag{3.1}$$

where the spectral parameter κ_N defines the natural sloshing frequencies $\sigma_N = \sqrt{\kappa_N}$ and Q_0, Σ_0 and S_0 are the mean liquid domain, free surface and wetted tank surface, respectively.

As we stated above, the nonlinear multimodal method requires the harmonic eigensolution $\{\varphi_N(t)\}$ which exactly (not approximately) satisfies the zero Neumann condition on the (mean) wetted tank surface. This solution cannot be expressed in terms of spherical functions whose Neumann traces on the spherical tank surface constitute a smooth orthogonal functional basis. How to get the required analytically approximate natural sloshing modes $\{\varphi_N(t)\}$ has been an old problem among scientists dealing with analytically oriented approaches to sloshing. Appropriate solutions were proposed by Barnyak *et al.* (2011) and Faltinsen & Timokha (2012). These solutions are given in the cylindrical coordinate system $(x_* = r_* \cos\theta, y_* = r_* \sin\theta, z_* = z)$, namely,

$$\begin{gathered} \varphi_N = \phi^*_{Mi}(r_*, z)\cos(M\theta), \quad M = 0, 1, \ldots \quad \text{or} \\ \phi^*_{mi}(r_*, z)\sin(m\theta), \quad m = 1, \ldots; \ i = 1, \ldots, \end{gathered} \tag{3.2}$$

where $N = (Mi)$ or $N = (mi)$. The capital letter implies the change from zero to infinity, but lower case indexes mean the change from one to infinity.

Except for the axisymmetric modes with $M = 0$, there are two cos and sin modes for each non-dimensional natural sloshing frequency $\sigma_{mi} = \sqrt{\kappa_{mi}}$. Index i

https://doi.org/10.1017/jfm.2012.635 Published online by Cambridge University Press

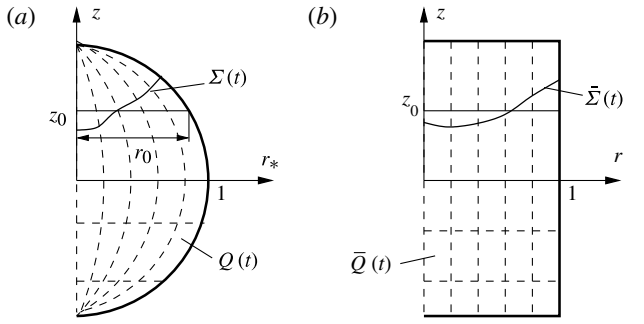


FIGURE 2. Transformation of the meridional cross-section from the physical space (a) to the transformed space (b).

enumerates the natural modes and frequencies for the same wavenumber in the angular direction which are characterized by different wave profiles in the radial direction. Employing (3.2) rewrites (2.5) in the form

$$\Phi(r_*,\theta,z,t)=\dot\eta_1(t)r_*\cos\theta+\dot\eta_2(t)r_*\sin\theta+\sum_{Mi}P_{Mi}(t)\phi^*_{Mi}(r_*,z)\cos(M\theta)$$
$$+\sum_{mi}R_{mi}(t)\phi^*_{mi}(r_*,z)\sin(m\theta). \tag{3.3}$$

3.2. *Modal representation of the free surface*

When dealing with vertical walls in a neighbourhood of the mean free surface, equation (2.3) can be written in the form $Z=z_*-\sum_N\beta_N f_N(x_*,y_*)$ where $\{f_N(x_*,y_*)\}$ is an orthogonal basis (normally, $f_N(x_*,y_*)=\varphi_N(x_*,y_*,z_0)$) on the mean free surface Σ_0 and domain of definition of $\{f_N(x,y)\}$ is time independent. This representation is not possible for the studied spherical shape in Cartesian, cylindrical and spherical coordinate systems. Therefore, we need a curvilinear coordinate system making the single-valued form of Z possible. Appropriate transformations to curvilinear coordinate systems were called the non-conformal mapping technique by Lukovsky (1975) and Lukovsky & Timokha (2002). An assumption is that overturning waves do not occur.

Following Lukovsky (1975) we introduce the transformation $r_*=r\sqrt{1-z^2}$ of the radial coordinate implying that the meridional tank cross-section maps to a rectangle as shown in figure 2. The transformed free surface $\bar\Sigma(t)$ admits then the needed single-valued representation

$$z=z_0+r_0\zeta(r,\theta,t)\Longrightarrow Z=z_*-z_0-r_0\zeta\left(\frac{r_*}{\sqrt{1-z^2}},\theta,t\right)=0, \tag{3.4}$$

defining, thereby, a special class of functions Z (definitions for z_0 and r_0 are given in figure 2) and leading to the modal representation

$$\zeta(r,\theta,t)=G(t)+\sum_{Mi}p_{Mi}(t)f_{Mi}(r)\cos(M\theta)+\sum_{mi}r_{mi}(t)f_{mi}(r)\sin(m\theta), \tag{3.5}$$

where $f_{mi}(r)=\phi^*_{mi}(rr_0,z_0)$. According to the corresponding spectral theorem on the natural linear sloshing modes (e.g. Eastham 1962; Morand & Ohayon 1995), the functional set $\{1,f_{Mi}(r)\cos(M\theta),f_{mi}(r)\sin(m\theta)\}$ constitutes an orthogonal basis

https://doi.org/10.1017/jfm.2012.635 Published online by Cambridge University Press

on the unit-radius circle. The orthogonality condition $\int_0^1 r f_{mi} f_{mj}\,\mathrm{d}r = \delta_{ij}$ yields the normalization

$$\phi^*_{mi}(r_*, z) := \frac{\phi^*_{mi}(r_*, z)}{\sqrt{\displaystyle\int_0^1 r\,(\phi^*_{mi}(rr_0, z_0))^2\,\mathrm{d}r\,\mathrm{sgn}(\phi_{mi}(r_0, z_0))}}. \tag{3.6}$$

The following identity

$$\int_{Q(t)} \mathscr{F}(x_*, y_*, z_*)\,\mathrm{d}x_*\,\mathrm{d}y_*\,\mathrm{d}z_* = \int_0^1 \int_{-\pi}^{\pi} r \int_{-1}^{z_0 + r_0\zeta} (1 - z^2)\mathscr{F}(r\sqrt{1 - z^2}\cos\theta, r\sqrt{1 - z^2}\sin\theta, z)\,\mathrm{d}z\,\mathrm{d}\theta\,\mathrm{d}r \tag{3.7}$$

is valid for arbitrary function $\mathscr{F}$. When $\mathscr{F} \equiv 1$, equation (2.4) leads to the volume conservation condition

$$\int_0^1 \int_{-\pi}^{\pi} r \left[r_0\zeta - z_0\zeta^2 - \frac{1}{3} r_0\zeta^3 \right] \mathrm{d}\theta\,\mathrm{d}r = 0 \tag{3.8}$$

in terms of ζ introduced in (3.4).

Condition (3.8) can be considered as a holonomic constraint with respect to the generalized coordinates p_{Mi} and r_{mi}. The constraint can be resolved at the zero (trivial) solution (unperturbed free surface) by using the implicit function theorem. This gives $G(t)$ as a function of other generalized coordinates

$$\begin{aligned} G(t) = G(\{p_{Mi}\}; \{r_{mi}\}) = {} & \underbrace{\frac{z_0}{r_0}\left[\sum_{Mi} \frac{\Lambda_{MM}}{\pi} p^2_{Mi} + \sum_{mi} r^2_{mi} \right]}_{G_2(t)} \\ & + \underbrace{\frac{1}{3\pi}\left[\sum_{MLNijk} \Lambda_{MLN,}\,\lambda_{(Mi)(Lj)(Nk)} p_{Mi} p_{Lj} p_{Nk} + 3 \sum_{Mlnijk} \Lambda_{M,ln}\lambda_{(Mi)(lj)(nk)} p_{Mi} r_{lj} r_{nk} \right]}_{G_3(t)} \\ & + \underbrace{\frac{z_0}{r_0}\left(1 + \frac{z_0^2}{r_0^2}\right)\left[\sum_{Mi} \frac{\Lambda_{MM}}{\pi} p^2_{Mi} + \sum_{mi} r^2_{mi} \right]^2}_{G_4(t) = \dfrac{r_0}{z_0}\left(1 + \dfrac{z_0^2}{r_0^2}\right)[G_2(t)]^2} + G_5(t) + \cdots, \end{aligned} \tag{3.9}$$

where $\{G_k(t)\}$ denote the k-order polynomial terms with respect to the generalized coordinates $\{p_{Mi}, r_{mi}\}$ and the coefficients Λ and λ are defined by formulas (A 1) and (A 3).

3.3. *Kinematic and dynamic equations*

Accounting for (3.3) and (3.5), modal (2.6) and (2.7) can be rewritten in a more appropriate form. The kinematic modal equations (2.6) take the form

$$\sum_{Mn} \frac{\partial A^p_{Ab}}{\partial p_{Mn}} \dot{p}_{Mn} + \sum_{mn} \frac{\partial A^p_{Ab}}{\partial r_{mn}} \dot{r}_{mn} = \sum_{Mn} A^{pp}_{(Ab)(Mn)} P_{Mn} + \sum_{mn} A^{pr}_{(Ab),(mn)} R_{mn}, \tag{3.10a}$$

https://doi.org/10.1017/jfm.2012.635 Published online by Cambridge University Press

$$\sum_{Mn}\frac{\partial A^{r}_{ab}}{\partial p_{Mn}}\dot{p}_{Mn}+\sum_{mn}\frac{\partial A^{r}_{ab}}{\partial r_{mn}}\dot{r}_{mn}=\sum_{Mn}A^{pr}_{(Mn),(ab)}P_{Mn}+\sum_{mn}A^{rr}_{(ab)(mn)}R_{mn} \tag{3.10b}$$

and the dynamic modal equations (2.7) are

$$\sum_{Mn}\frac{\partial A^{p}_{Mn}}{\partial p_{Ab}}\dot{P}_{Mn}+\sum_{mn}\frac{\partial A^{r}_{mn}}{\partial p_{Ab}}\dot{R}_{mn}+\frac{1}{2}\sum_{MLnk}\frac{\partial A^{pp}_{(Mn)(Lk)}}{\partial p_{Ab}}P_{Mn}P_{Lk}+\frac{1}{2}\sum_{mlnk}\frac{\partial A^{rr}_{(mn)(lk)}}{\partial p_{Ab}}R_{mn}R_{lk}$$
$$+\sum_{Mlnk}\frac{\partial A^{pr}_{(Mn),(lk)}}{\partial p_{Ab}}P_{Mn}R_{lk}+\frac{\partial l_3}{\partial p_{Ab}}+\ddot{\eta}_1\frac{\partial l_1}{\partial p_{Ab}}+\ddot{\eta}_2\frac{\partial l_2}{\partial p_{Ab}}=0, \tag{3.11a}$$

$$\sum_{Mn}\frac{\partial A^{p}_{Mn}}{\partial r_{ab}}\dot{P}_{Mn}+\sum_{mn}\frac{\partial A^{r}_{mn}}{\partial r_{ab}}\dot{R}_{mn}+\frac{1}{2}\sum_{MLnk}\frac{\partial A^{pp}_{(Mn)(Lk)}}{\partial r_{ab}}P_{Mn}P_{Lk}+\frac{1}{2}\sum_{mlnk}\frac{\partial A^{rr}_{(mn)(lk)}}{\partial r_{ab}}R_{mn}R_{lk}$$
$$+\sum_{Mlnk}\frac{\partial A^{pr}_{(Mn),(lk)}}{\partial r_{ab}}P_{Mn}R_{lk}+\frac{\partial l_3}{\partial r_{ab}}+\ddot{\eta}_1\frac{\partial l_1}{\partial r_{ab}}+\ddot{\eta}_2\frac{\partial l_2}{\partial r_{ab}}=0, \tag{3.11b}$$

where $A=0,1,\ldots$ and $a,b=1,2,\ldots$. Moreover, using (3.4) and (3.5) within (3.9) and accounting for (3.7) gives the following explicit expressions for integrals (2.8):

$$A^{p}_{Ab}=\int_0^1 r\int_{-\pi}^{\pi}\cos(A\theta)\mathscr{G}^{(0)}_{Ab}(r,\theta;p_{Ij}(t);r_{ij}(t))\,\mathrm{d}\theta\,\mathrm{d}r, \tag{3.12a}$$

$$A^{r}_{ab}=\int_0^1 r\int_{-\pi}^{\pi}\sin(a\theta)\mathscr{G}^{(0)}_{ab}(r,\theta;p_{Ij}(t);r_{ij}(t))\,\mathrm{d}\theta\,\mathrm{d}r, \tag{3.12b}$$

$$A^{pp}_{(Ab)(Mn)}=\int_0^1 r\int_{-\pi}^{\pi}\Big\{\cos(A\theta)\cos(M\theta)\ \mathscr{G}^{(1)}_{(Ab)(Mn)}(r,\theta;p_{Ij}(t);r_{ij}(t))$$
$$+\sin(A\theta)\sin(M\theta)\ \mathscr{G}^{(2)}_{(Ab)(Mn)}(r,\theta;p_{Ij}(t);r_{ij}(t))\Big\}\,\mathrm{d}\theta\,\mathrm{d}r, \tag{3.13a}$$

$$A^{rr}_{(ab)(mn)}=\int_0^1 r\int_{-\pi}^{\pi}\Big\{\sin(a\theta)\sin(m\theta)\ \mathscr{G}^{(1)}_{(Ab)(Mn)}(r,\theta;p_{Ij}(t);r_{ij}(t))$$
$$+\cos(a\theta)\cos(m\theta)\ \mathscr{G}^{(2)}_{(Ab)(Mn)}(r,\theta;p_{Ij}(t);r_{ij}(t))\Big\}\,\mathrm{d}\theta\,\mathrm{d}r, \tag{3.13b}$$

$$A^{pr}_{(Ab),(mn)}=\int_0^1 r\int_{-\pi}^{\pi}\Big\{\cos(A\theta)\sin(m\theta)\ \mathscr{G}^{(1)}_{(Ab)(Mn)}(r,\theta;p_{Ij}(t);r_{ij}(t))$$
$$-\sin(A\theta)\cos(m\theta)\ \mathscr{G}^{(2)}_{(Ab)(Mn)}(r,\theta;p_{Ij}(t);r_{ij}(t))\Big\}\,\mathrm{d}\theta\,\mathrm{d}r, \tag{3.13c}$$

where

$$\mathscr{G}^{(0)}_{ab}(r,\theta;p_{Ij}(t);r_{ij}(t))=\int_{-1}^{z_0+r_0\zeta(r,\theta;p_{Ij}(t);r_{ij}(t))}(1-z^2)\,\phi^{*}_{ab}\left(r\sqrt{1-z^2},z\right)\mathrm{d}z, \tag{3.14a}$$

$$\mathscr{G}^{(1)}_{(ab)(cd)}(r,\theta;p_{Ij}(t);r_{ij}(t))=\int_{-1}^{z_0+r_0\zeta(r,\theta;p_{Ij}(t);r_{ij}(t))}(1-z^2)$$
$$\times\left[\frac{\partial\phi^{*}_{ab}}{\partial r_*}\frac{\partial\phi^{*}_{cd}}{\partial r_*}+\frac{\partial\phi^{*}_{ab}}{\partial z_*}\frac{\partial\phi^{*}_{cd}}{\partial z_*}\right]_{(r\sqrt{1-z^2},z)}\mathrm{d}z, \tag{3.14b}$$

$$\mathscr{G}^{(2)}_{(ab)(cd)}(r,\theta;p_{Ij}(t);r_{ij}(t))=\frac{1}{r^2}\int_{-1}^{z_0+r_0\zeta(r,\theta;p_{Ij}(t);r_{ij}(t))}\left[\phi^{*}_{ab}\phi^{*}_{cd}\right]_{(r\sqrt{1-z^2},z)}\mathrm{d}z \tag{3.14c}$$

https://doi.org/10.1017/jfm.2012.635 Published online by Cambridge University Press

and

$$l_3 = \int_0^1 \int_{-\pi}^{\pi} \int_{-1}^{z_0 + r_0 \zeta(r,\theta;p_{Ij}(t);r_{ij}(t))} rz(1-z^2)\ \mathrm{d}z\,\mathrm{d}\theta\,\mathrm{d}r, \tag{3.15a}$$

$$l_2 = r_0 \int_0^1 \int_{-\pi}^{\pi} \int_{-1}^{z_0 + r_0 \zeta(r,\theta;p_{Ij}(t);r_{ij}(t))} r^2(1-z^2)\sin\theta\ \mathrm{d}z\,\mathrm{d}\theta\,\mathrm{d}r, \tag{3.15b}$$

$$l_1 = r_0 \int_0^1 \int_{-\pi}^{\pi} \int_{-1}^{z_0 + r_0 \zeta(r,\theta;p_{Ij}(t);r_{ij}(t))} r^2(1-z^2)\cos\theta\ \mathrm{d}z\,\mathrm{d}\theta\,\mathrm{d}r. \tag{3.15c}$$

After adding the initial conditions for the generalized coordinates p_{Mi}, r_{mj} and velocities P_{Mi}, R_{mj}, the system of ordinary differential equations (3.10) and (3.11) can be used for direct time simulations using the method of Perko (Moore & Perko 1964; Perko 1969; La Rocca *et al.* 2000).

3.4. *A weakly nonlinear form of the general modal equations*

Remembering the weakly nonlinear modal equations by Faltinsen & Timokha (2001), Faltinsen *et al.* (2003, 2005*b*) and Ikeda *et al.* (2012), we will use (3.10) and (3.11) to find the generalized velocities as functions of the generalized coordinates and their time derivatives and, furthermore, derive the third-order modal equations with respect to p_{Mi} and r_{mi}. The procedure assumes

$$p_{Mi} \sim P_{Mi} \sim r_{mi} \sim R_{mi} = O(\epsilon^{1/3}), \tag{3.16}$$

where $\epsilon \ll 1$ is the order of the non-dimensional external forcing magnitude,

$$\eta_1(t) \sim \eta_2(t) = O(\epsilon), \tag{3.17}$$

and requires to neglect the $o(\epsilon)$ quantities.

The derivation steps are described in appendix A. First, we find A^p_{Ab} and A^r_{ab} up to cubic terms (§ A.1) and keep quadratic terms in (3.13*a*) (§ A.2). Second, we asymptotically resolve the kinematic modal (3.10) with respect to the generalized velocities

$$\begin{aligned} P_{Ab} = {} & \frac{r_0}{\kappa_{Ab}}\dot{p}_{Ab} + \sum_{MNij} V^{pp}_{(Mi),(Nj),(Ab)}\dot{p}_{Mi}p_{Nj} + \sum_{mnij} V^{rr}_{(mi),(nj),(Ab)}\dot{r}_{mi}r_{nj} \\ & + \sum_{MNKijl} V^{ppp}_{(Mi),(Nj),(Kl),(Ab)}\dot{p}_{Mi}p_{Nj}p_{Kl} + \sum_{Mnkijl} V^{prr}_{(Mi),(nj),(kl),(Ab)}\dot{p}_{Mi}r_{nj}r_{kl} \\ & + \sum_{Mnkijl} V^{rpr}_{(nj),(Mi),(kl),(Ab)}\dot{r}_{nj}p_{Mi}r_{kl}, \end{aligned} \tag{3.18a}$$

$$\begin{aligned} R_{ab} = {} & \frac{r_0}{\kappa_{ab}}\dot{r}_{ab} + \sum_{Mnij} V^{pr}_{(Mi),(nj),(ab)}\dot{p}_{Mi}r_{nj} + \sum_{Mnij} V^{rp}_{(nj),(Mi),(ab)}\dot{r}_{nj}p_{Mi} \\ & + \sum_{mnkijl} V^{rrr}_{(mi),(nj),(kl),(ab)}\dot{r}_{mi}r_{nj}r_{kl} + \sum_{MNkijl} V^{rpp}_{(kl),(Mi),(Nj),(ab)}\dot{r}_{kl}p_{Mi}p_{Nj} \\ & + \sum_{MNkijl} V^{ppr}_{(Mi),(Nj),(kl),(ab)}\dot{p}_{Mi}p_{Nj}r_{kl}. \end{aligned} \tag{3.18b}$$

https://doi.org/10.1017/jfm.2012.635 Published online by Cambridge University Press

Explicit formulas for the V-coefficients are given in § A.3 and, finally, § A.4 derives the weakly nonlinear modal equations

$$\sum_{Mi}\ddot{p}_{Mi}\left[\delta_{ME}\delta_{if}+\sum_{Nj}d^{pp,(Ef)}_{(Mi),(Nj)}p_{Nj}+\sum_{NKjl}d^{ppp,(Ef)}_{(Mi),(Nj),(Kl)}p_{Nj}p_{Kl}\right.$$
$$\left.+\sum_{nkjl}d^{prr,(Ef)}_{(Mi),(nj),(kl)}r_{nj}r_{kl}\right]+\sum_{mnij}\ddot{r}_{mi}r_{nj}\left[d^{rr,(Ef)}_{(mi),(nj)}+\sum_{Kl}d^{rrp,(Ef)}_{(mi),(nj),(Kl)}p_{Kl}\right]$$
$$+\sum_{MNij}\dot{p}_{Mi}\dot{p}_{Nj}\left[t^{pp,(Ef)}_{(Mi),(Nj)}+\sum_{Kl}t^{ppp,(Ef)}_{(Mi),(Nj),(Kl)}p_{Kl}\right]+\sum_{Mnkijl}t^{prr,(Ef)}_{(Mi),(nj),(kl)}\dot{p}_{Mi}\dot{r}_{nj}r_{kl}$$
$$+\sum_{mnij}\dot{r}_{mi}\dot{r}_{nj}\left[t^{rr,(Ef)}_{(mi),(nj)}+\sum_{Kl}t^{rrp,(Ef)}_{(mi),(nj),(Kl)}p_{Kl}\right]$$
$$+\sum_{Mi}p_{Mi}\left[\kappa_{Ef}\delta_{ME}\delta_{if}+\sum_{Nj}g^{pp,(Ef)}_{(Mi)(Nj)}p_{Nj}+\sum_{NKil}g^{ppp,(Ef)}_{(Mi)(Nj)(Kl)}p_{Nj}p_{Kl}\right.$$
$$\left.+\sum_{nkjl}g^{prr,(Ef)}_{(Mi),(nj)(kl)}r_{nj}r_{kl}\right]+\sum_{mnij}g^{rr,(Ef)}_{(mi)(nj)}r_{mi}r_{nj}=-\ddot{\eta}_1(t)\delta_{1E}e_f; \tag{3.19a}$$

$$\sum_{Mnij}\ddot{p}_{Mi}r_{nj}\left[d^{pr,(ef)}_{(Mi),(nj)}+\sum_{Kl}d^{prp,(ef)}_{(Mi),(nj),(Kl)}p_{Kl}\right]+\sum_{mi}\ddot{r}_{mi}\left[\delta_{me}\delta_{ij}+\sum_{Nj}d^{rp,(ef)}_{(mi),(Nj)}p_{Nj}\right.$$
$$\left.+\sum_{NKjl}d^{rpp,(ef)}_{(mi),(Nj),(Kl)}p_{Nj}p_{Kl}+\sum_{nkjl}d^{rrr,(ef)}_{(mi),(nj),(kl)}r_{nj}r_{kl}\right]$$
$$+\sum_{Mnij}\dot{p}_{Mi}\dot{r}_{nj}\left[t^{pr,(ef)}_{(Mi),(nj)}+\sum_{Kl}t^{prp,(ef)}_{(Mi),(nj),(Kl)}p_{Kl}\right]+\sum_{MNkijl}t^{ppr,(ef)}_{(Mi),(Nj),(kl)}\dot{p}_{Mi}\dot{p}_{Nj}r_{kl}$$
$$+\sum_{mnkijl}t^{rrr,(ef)}_{(mi),(nj),(kl)}\dot{r}_{mi}\dot{r}_{nj}r_{kl}+\sum_{mi}r_{mi}\left[\kappa_{ef}\delta_{me}\delta_{if}+\sum_{Nj}g^{rp,(ef)}_{(mi),(Nj)}p_{Nj}\right.$$
$$\left.+\sum_{NKjl}g^{rpp,(ef)}_{(mi),(Nj)(Kl)}p_{Nj}p_{Kl}+\sum_{nkij}g^{rrr,(ef)}_{(mi)(nj)(kl)}r_{nj}r_{kl}\right]=-\ddot{\eta}_2\delta_{1e}e_f. \tag{3.19b}$$

Expressions for the hydrodynamic coefficients in appendix A appear more complicated than those in analogous weakly nonlinear modal equations by Faltinsen *et al.* (2003) and Love & Tait (2010, 2011) derived for a square-base tank. However, they are the same from an algorithmic point of view. The only difference is that computations involve analytically approximate $\phi^*_{Mi}(r_*, z)$ coming from the paper by Faltinsen & Timokha (2012).

The modal equations (3.19) can be simplified by noting that many of the hydrodynamic coefficients are zeros and by selecting the first-, second- and third-order generalized coordinates p_{Mi} and r_{mi} based on a set of specific asymptotic relationships between the generalized coordinates.

https://doi.org/10.1017/jfm.2012.635 Published online by Cambridge University Press

4. The Moiseev–Narimanov asymptotic multimodal analysis

4.1. *Introducing the Moiseev–Narimanov asymptotic relationships*

Assuming that (*a*) the $O(\epsilon)$-order small-amplitude harmonic excitations with the forcing frequency σ close to the lowest natural sloshing frequency (here, $\sqrt{\kappa_{11}}$) and (*b*) there are no secondary resonances and other small non-dimensional parameters, e.g. shallow liquid depth, Moiseev (1958): (i) showed that the dominant sloshing response is of the order $O(\epsilon^{1/3})$ contributed by the primary excited lowest mode (here, the two modes associated with p_{11} and r_{11}); and (ii) derived a necessary (secular) condition of the steady-state (time-periodic) solution to exist.

The Moiseev steady-state solution yields special asymptotic intermodal relations which are a background for multimodal analysis and other analytical approaches to nonlinear sloshing (see, review by Faltinsen & Timokha 2009). Similar relations were proposed by Narimanov (1957) for axisymmetric tanks and arbitrary almost-periodic motions whose mean frequency is close to the lowest natural sloshing frequency. For the axisymmetric tanks, due to trigonometric formulas with respect to the angular coordinate, the Moiseev–Narimanov relations read as

$$\left.\begin{array}{l} p_{11}\sim r_{11}=O(\epsilon^{1/3}),\quad p_{0j}\sim p_{2j}\sim r_{2j}=O(\epsilon^{2/3}),\\ r_{1(j+1)}\sim p_{1(j+1)}\sim p_{3j}\sim r_{3j}=O(\epsilon),\quad j=1,2,\ldots. \end{array}\right\} \tag{4.1}$$

The other remaining generalized coordinates are of the order $o(\epsilon)$ and, therefore, they are not involved in the third-order nonlinear interaction.

Examples of approximate weakly nonlinear modal systems for upright circular cylindrical tanks based on (4.1) can be found in the papers by Miles (1984*a*,*b*), Lukovsky (1990), Lukovsky & Timokha (1995), Gavrilyuk *et al.* (2000, 2007), Ikeda & Ibrahim (2005), Lukovsky *et al.* (2012) and Takahara & Kimura (2012).

4.2. *Modal equations*

Tedious but straightforward derivations show that the Moiseev–Narimanov modal equations for the spherical tank take the form

$$\begin{aligned} &\ddot p_{11}+\sigma_{11}^2p_{11}+d_1p_{11}\left(\ddot p_{11}p_{11}+\ddot r_{11}r_{11}+\dot p_{11}^2+\dot r_{11}^2\right)+d_2\left[r_{11}(\ddot p_{11}r_{11}-\ddot r_{11}p_{11})\right.\\ &\quad\left.+2\dot r_{11}(\dot p_{11}r_{11}-\dot r_{11}p_{11})\right]+\sigma_{11}^2\mathscr{G}_1p_{11}\underline{\left[p_{11}^2+r_{11}^2\right]}\\ &\quad+\sum_{j=1}^{\infty}\left[d_3^{(j)}(\ddot p_{11}p_{2j}+\ddot r_{11}r_{2j}+\dot p_{11}\dot p_{2j}+\dot r_{11}\dot r_{2j})\right.\\ &\quad+d_4^{(j)}(\ddot p_{2j}p_{11}+\ddot r_{2j}r_{11})+d_5^{(j)}\left(\ddot p_{11}p_{0j}+\dot p_{11}\dot p_{0j}\right)\\ &\quad\left.+d_6^{(j)}\ddot p_{0j}p_{11}+\sigma_{11}^2\left(\mathscr{G}_2^{(j)}\underline{(p_{11}p_{2j}+r_{11}r_{2j})}+\mathscr{G}_3^{(j)}\underline{p_{0j}p_{11}}\right)\right]=-e_1\,\ddot\eta_1, \end{aligned} \tag{4.2a}$$

$$\begin{aligned} &\ddot r_{11}+\sigma_{11}^2r_{11}+d_1r_{11}\left[\ddot p_{11}p_{11}+\ddot r_{11}r_{11}+\dot p_{11}^2+\dot r_{11}^2\right]+d_2\left[p_{11}(\ddot r_{11}p_{11}-\ddot p_{11}r_{11})\right.\\ &\quad\left.+2\dot p_{11}(\dot r_{11}p_{11}-\dot p_{11}r_{11})\right]+\sigma_{11}^2\mathscr{G}_1r_{11}\underline{\left[p_{11}^2+r_{11}^2\right]}\\ &\quad+\sum_{j=1}^{\infty}\left[d_3^{(j)}\left(\ddot p_{11}r_{2j}-\ddot r_{11}p_{2j}+\dot p_{11}\dot r_{2j}-\dot p_{2j}\dot r_{11}\right)\right.\\ &\quad+d_4^{(j)}(\ddot r_{2j}p_{11}-\ddot p_{2j}r_{11})+d_5^{(j)}(\ddot r_{11}p_{0j}+\dot r_{11}\dot p_{0j})\\ &\quad\left.+d_6^{(j)}\ddot p_{0j}r_{11}+\sigma_{11}^2\left(\mathscr{G}_2^{(j)}\underline{(p_{11}r_{2j}-p_{2j}r_{11})}+\mathscr{G}_3^{(j)}\underline{p_{0j}r_{11}}\right)\right]=-e_1\,\ddot\eta_2; \end{aligned} \tag{4.2b}$$

https://doi.org/10.1017/jfm.2012.635 Published online by Cambridge University Press

$$\ddot{p}_{2k}+\sigma_{2k}^2 p_{2k}+d_{7,k}(\dot{p}_{11}^2-\dot{r}_{11}^2)+d_{9,k}(\ddot{p}_{11}p_{11}-\ddot{r}_{11}r_{11})+\sigma_{2k}^2\mathscr{G}_{4,k}\underline{(p_{11}^2-r_{11}^2)}=0, \quad (4.3a)$$

$$\ddot{r}_{2k}+\sigma_{2k}^2 r_{2k}+2d_{7,k}\dot{p}_{11}\dot{r}_{11}+d_{9,k}(\ddot{p}_{11}r_{11}+\ddot{r}_{11}p_{11})+2\sigma_{2k}^2\mathscr{G}_{4,k}\underline{p_{11}r_{11}}=0, \quad (4.3b)$$

$$\ddot{p}_{0k}+\sigma_{0k}^2 p_{0k}+d_{8,k}(\dot{p}_{11}^2+\dot{r}_{11}^2)+d_{10,k}(\ddot{p}_{11}p_{11}+\ddot{r}_{11}r_{11})+\sigma_{0k}^2\mathscr{G}_{5,k}\underline{(p_{11}^2+r_{11}^2)}=0; \quad (4.3c)$$

$$\begin{aligned}&\ddot{p}_{3k}+\sigma_{3k}^2 p_{3k}+d_{11,k}\left[\ddot{p}_{11}(p_{11}^2-r_{11}^2)-2p_{11}r_{11}\ddot{r}_{11}\right]+d_{12,k}\left[p_{11}(\dot{p}_{11}^2-\dot{r}_{11}^2)-2r_{11}\dot{p}_{11}\dot{r}_{11}\right]\\&\quad+\sigma_{3k}^2\mathscr{G}_{6,k}\underline{p_{11}(p_{11}^2-3r_{11}^2)}+\sum_{j=1}^{\infty}\Big[d_{13,k}^{(j)}(\ddot{p}_{11}p_{2j}-\ddot{r}_{11}r_{2j})+d_{14,k}^{(j)}(\ddot{p}_{2j}p_{11}-\ddot{r}_{2j}r_{11})\\&\quad+d_{15,k}^{(j)}(\dot{p}_{2j}\dot{p}_{11}-\dot{r}_{2j}\dot{r}_{11})+\sigma_{3k}^2\mathscr{G}_{7,k}^{(j)}\underline{(p_{11}p_{2j}-r_{11}r_{2j})}\Big]=0,\end{aligned} \quad (4.4a)$$

$$\begin{aligned}&\ddot{r}_{3k}+\sigma_{3k}^2 r_{3k}+d_{11,k}\left[\ddot{r}_{11}(p_{11}^2-r_{11}^2)+2p_{11}r_{11}\ddot{p}_{11}\right]+d_{12,k}\left[r_{11}(\dot{p}_{11}^2-\dot{r}_{11}^2)+2p_{11}\dot{p}_{11}\dot{r}_{11}\right]\\&\quad+\sigma_{3k}^2\mathscr{G}_{6,k}\underline{r_{11}(3p_{11}^2-r_{11}^2)}+\sum_{j=1}^{\infty}\Big[d_{13,k}^{(j)}(\ddot{p}_{11}r_{2j}+\ddot{r}_{11}p_{2j})+d_{14,k}^{(j)}(\ddot{p}_{2j}r_{11}+\ddot{r}_{2j}p_{11})\\&\quad+d_{15,k}^{(j)}(\dot{p}_{2j}\dot{r}_{11}+\dot{r}_{2j}\dot{p}_{11})+\sigma_{3k}^2\mathscr{G}_{7,k}^{(j)}\underline{(p_{11}r_{2j}+r_{11}p_{2j})}\Big]=0,\ \ k=1,2,\ldots;\end{aligned} \quad (4.4b)$$

$$\begin{aligned}&\ddot{p}_{1n}+\sigma_{1n}^2 p_{1n}+d_{16,n}(\ddot{p}_{11}p_{11}^2+r_{11}p_{11}\ddot{r}_{11})+d_{17,n}(\ddot{p}_{11}r_{11}^2-r_{11}p_{11}\ddot{r}_{11})\\&\quad+d_{18,n}p_{11}(\dot{p}_{11}^2+\dot{r}_{11}^2)+d_{19,n}(r_{11}\dot{p}_{11}\dot{r}_{11}-p_{11}\dot{r}_{11}^2)+\sigma_{1n}^2\mathscr{G}_{1,n}\underline{p_{11}\left[p_{11}^2+r_{11}^2\right]}\\&\quad+\sum_{j=1}^{\infty}\Big[d_{20,n}^{(j)}(\ddot{p}_{11}p_{2j}+\ddot{r}_{11}r_{2j})+d_{21,n}^{(j)}(p_{11}\ddot{p}_{2j}+r_{11}\ddot{r}_{2j})+d_{22,n}^{(j)}(\dot{p}_{11}\dot{p}_{2j}+\dot{r}_{11}\dot{r}_{2j})\\&\quad+d_{23,n}^{(j)}\ddot{p}_{11}p_{0j}+d_{24,n}^{(j)}p_{11}\ddot{p}_{0j}+d_{25,n}^{(j)}\dot{p}_{11}\dot{p}_{0j}+\sigma_{1n}^2\left(\mathscr{G}_{2,n}^{(j)}\underline{(p_{11}p_{2j}+r_{11}r_{2j})}+\mathscr{G}_{3,n}^{(j)}\underline{p_{11}p_{0j}}\right)\Big]\\&\quad=-e_n\ddot{\eta}_1,\end{aligned} \quad (4.5a)$$

$$\begin{aligned}&\ddot{r}_{1n}+\sigma_{1n}^2 r_{1n}+d_{16,n}(\ddot{r}_{11}r_{11}^2+r_{11}p_{11}\ddot{p}_{11})+d_{17,n}(\ddot{r}_{11}p_{11}^2-r_{11}p_{11}\ddot{p}_{11})\\&\quad+d_{18,n}r_{11}(\dot{p}_{11}^2+\dot{r}_{11}^2)+d_{19,n}(p_{11}\dot{p}_{11}\dot{r}_{11}-r_{11}\dot{p}_{11}^2)+\sigma_{1n}^2\mathscr{G}_{1,n}\underline{r_{11}\left[p_{11}^2+r_{11}^2\right]}\\&\quad+\sum_{j=1}^{\infty}\Big[d_{20,n}^{(j)}(\ddot{p}_{11}r_{2j}-\ddot{r}_{11}p_{2j})+d_{21,n}^{(j)}(p_{11}\ddot{r}_{2j}-r_{11}\ddot{p}_{2j})+d_{22,n}^{(j)}(\dot{p}_{11}\dot{r}_{2j}-\dot{r}_{11}\dot{p}_{2j})\\&\quad+d_{23,n}^{(j)}\ddot{r}_{11}p_{0j}+d_{24,n}^{(j)}r_{11}\ddot{p}_{0j}+d_{25,n}^{(j)}\dot{r}_{11}\dot{p}_{0j}+\sigma_{1n}^2\left(\mathscr{G}_{2,n}^{(j)}\underline{(p_{11}r_{2j}-r_{11}p_{2j})}+\mathscr{G}_{3,n}^{(j)}\underline{r_{11}p_{0j}}\right)\Big]\\&\quad=-e_n\ddot{\eta}_2,\quad n=2,3,\ldots,\end{aligned} \quad (4.5b)$$

where computational formulas for the hydrodynamic coefficients are collected in appendix B and $\sigma_{Mi}=\sqrt{\kappa_{Mi}}$ are the non-dimensional natural sloshing frequencies introduced in § 3.1. Specifically, the computational formulas contain infinite summations that are truncated by using a finite number of the second- and third-order modes indexed by i (here, $M=0,1,2,3$ and $m=1,2,3$) in modal representations (3.3) and (3.5). Calculations show that these coefficients rapidly converge for $0<h\lesssim 1$ so that taking from one to four elements by the index i provides stabilization of four to five significant figures. For $1\lesssim h\leqslant 2$, the convergence is slower but from four to eight summands by the number i still guarantee stabilization to three to four significant figures.

It is an amazing fact that except for the underlined quantities meaning a 'geometric nonlinearity', equations (4.2)–(4.5) have the same structure as the Moiseev–Narimanov

https://doi.org/10.1017/jfm.2012.635 Published online by Cambridge University Press

modal systems for sloshing in an upright circular cylindrical tank (Lukovsky *et al.* 2012). Because the approximate five-dimensional system of modal equations by Gavrilyuk *et al.* (2005) for sloshing in a V-conical tank (with respect to $r_{11}, p_{11}, p_{01}, p_{21}$ and r_{21}) takes the same structure as the corresponding differential equations in (4.2)–(4.3), the differential equations (4.2)–(4.5) may be an invariant for any axisymmetric tanks. The tank geometry affects values of the hydrodynamic coefficients and natural frequencies but not the structure of the Moiseev–Narimanov modal equations.

The Moiseev–Narimanov modal system (4.2)–(4.5) can be equipped with the linear damping terms $-2\xi_{Mi}\sigma_{Mi}\dot{p}_{Mi}$ and $-2\xi_{mi}\sigma_{mi}\dot{r}_{mi}$ incorporated into the corresponding equations. Numerical simulations by Faltinsen *et al.* (2005*a*) showed for a square-base tank that those linear damping terms based on liquid bulk viscosity and laminar boundary layer flow at the tank walls have almost no influence on the periodic solutions. A reason is that the damping ratios ξ_{mi} are normally small, of the order of $O(\epsilon)$ (forcing magnitude), for realistic liquids and model tests in which nonlinear sloshing is observed and, as a consequence, $-2\xi_{Mi}\sigma_{Mi}\dot{p}_{Mi}$ and $-2\xi_{mi}\sigma_{mi}\dot{r}_{mi}$ are of the order $\lesssim O(\epsilon^{4/3})$ and should be omitted within the framework of the Moiseev–Narimanov asymptotics. Since the same can be stated for experiments by Sumner & Stofan (1963), which is our primary focus, the damping terms will furthermore be neglected which is appropriate as long as breaking waves do not occur.

4.3. *Steady-state (time-periodic) resonant wave regimes and their stability*

We consider a small-amplitude harmonic horizontal excitation that occurs, for brevity, along the Ox-axis, $\eta_1(t) = \eta_{1a}\cos(\sigma t)$ and $\eta_2(t) \equiv 0$. Following Faltinsen & Timokha (2009, chap. 9), one can construct an asymptotic steady-state solution in terms of

$$\epsilon^{1/3} = \eta_{1a}^{1/3} \ll 1. \tag{4.6}$$

For this purpose, we introduce the lowest-order quantities

$$p_{11} = A\cos(\sigma t) + \bar{A}\sin(\sigma t) + O(\epsilon), \quad r_{11} = \bar{B}\cos(\sigma t) + B\sin(\sigma t) + O(\epsilon) \tag{4.7}$$

where $A, \bar{A}, \bar{B}$ and B are the $O(\epsilon^{1/3})$-amplitude parameters. Inserting (4.7) into (4.3) gives

$$\begin{aligned} p_{0k} &= s_{0k}(A^2 + \bar{A}^2 + B^2 + \bar{B}^2) \\ &\quad + s_{1k}\left[(A^2 - \bar{A}^2 - B^2 + \bar{B}^2)\cos(2\sigma t) + 2(A\bar{A} + B\bar{B})\sin(2\sigma t)\right] + o(\epsilon), \quad (4.8a) \\ p_{2k} &= c_{0k}(A^2 + \bar{A}^2 - B^2 - \bar{B}^2) \\ &\quad + c_{1k}\left[(A^2 - \bar{A}^2 + B^2 - \bar{B}^2)\cos(2\sigma t) + 2(A\bar{A} - B\bar{B})\sin(2\sigma t)\right] + o(\epsilon), \quad (4.8b) \\ r_{2k} &= 2c_{0k}(A\bar{B} + B\bar{A}) + 2c_{1k} \\ &\quad \times \left[(A\bar{B} - B\bar{A})\cos(2\sigma t) + (AB + \bar{A}\bar{B})\sin(2\sigma t)\right] + o(\epsilon), \quad (4.8c) \end{aligned}$$

where

$$s_{0k} = \frac{1}{2}\left(\frac{d_{10,k} - d_{8,k}}{\bar{\sigma}_{0k}^2} - \mathscr{G}_{5,k}\right), \quad s_{1k} = \frac{d_{10,k} + d_{8,k} - \mathscr{G}_{5,k}\bar{\sigma}_{0k}^2}{2(\bar{\sigma}_{0k}^2 - 4)}, \quad \bar{\sigma}_{0k} = \frac{\sigma_{0k}}{\sigma}, \tag{4.9a}$$

$$c_{0k} = \frac{1}{2}\left(\frac{d_{9,k} - d_{7,k}}{\bar{\sigma}_{2k}^2} - \mathscr{G}_{4,k}\right), \quad c_{1k} = \frac{d_{9,k} + d_{7,k} - \mathscr{G}_{4,k}\bar{\sigma}_{2k}^2}{2(\bar{\sigma}_{2k}^2 - 4)}, \quad \bar{\sigma}_{2k} = \frac{\sigma_{2k}}{\sigma}. \tag{4.9b}$$

https://doi.org/10.1017/jfm.2012.635 Published online by Cambridge University Press

Substituting (4.7) and (4.8) into (4.2) and gathering the lowest-order terms at $\cos(\sigma t)$ and $\sin(\sigma t)$ leads to the secular equations with respect to the dominant amplitude parameters

$$\begin{cases} A\left[(\bar\sigma_{11}^2-1)+m_1(A^2+\bar A^2+\bar B^2)+m_3B^2\right]+(m_1-m_3)\bar A\bar BB=e_1\eta_{1a},\\ \bar A\left[(\bar\sigma_{11}^2-1)+m_1(A^2+\bar A^2+B^2)+m_3\bar B^2\right]+(m_1-m_3)A\bar BB=0,\\ \bar B\left[(\bar\sigma_{11}^2-1)+m_1(B^2+\bar B^2+A^2)+m_3\bar A^2\right]+(m_1-m_3)\bar AAB=0,\\ B\left[(\bar\sigma_{11}^2-1)+m_1(B^2+\bar B^2+\bar A^2)+m_3A^2\right]+(m_1-m_3)\bar A A\bar B=0. \end{cases} \tag{4.10}$$

Here, $\bar\sigma_{11}=\sigma_{11}/\sigma$ and

$$\begin{aligned} m_1(\bar\sigma_{11}) &= -S_0^{d_5}+\tfrac12 S_1^{d_5}-C_0^{d_3}+\tfrac12 C_1^{d_3}-2C_1^{d_4}-2S_1^{d_6}-\tfrac12 d_1\\ &\quad+\bar\sigma_{11}^2\left[S_0^{G_3}+\tfrac12 S_1^{G_3}+C_0^{G_2}+\tfrac12 C_1^{G_2}+\tfrac34\mathscr{G}_1\right], \end{aligned} \tag{4.11a}$$

$$\begin{aligned} m_3(\bar\sigma_{11}) &= -S_0^{d_5}-\tfrac12 S_1^{d_5}+\tfrac32 C_1^{d_3}+C_0^{d_3}-6C_1^{d_4}+2S_1^{d_6}-2d_2+\tfrac12 d_1\\ &\quad+\bar\sigma_{11}^2\left[S_0^{G_3}-\tfrac12 S_1^{G_3}-C_0^{G_2}+\tfrac32 C_1^{G_2}+\tfrac14\mathscr{G}_1\right] \end{aligned} \tag{4.11b}$$

within

$$S_a^{d_n}=\sum_{j=1}^{\infty} d_b^{(j)}s_{aj},\quad C_a^{d_n}=\sum_{j=1}^{\infty} d_b^{(j)}C_{aj},\quad S_a^{G_l}=\sum_{j=1}^{\infty}\mathscr{G}_l^{(j)}s_{aj},\quad C_a^{G_l}=\sum_{j=1}^{\infty}\mathscr{G}_l^{(j)}s_{aj} \tag{4.12}$$

for $a=0,1$, $l=2,3$ and $b=3,\dots,6$.

The secular equations (4.10) have the same structure as those appearing for studying the time-periodic resonant sloshing in a circular-base tank. As a consequence, response curves and bifurcation points following from (4.10) should be qualitatively identical to those described by Miles (1984*b*,*a*) and Gavrilyuk *et al.* (2000, 2007).

Getting a solution to (4.10) and gathering the terms in the front of the $\sin(3\sigma t)$ and $\cos(3\sigma t)$ harmonics make it possible to find the $O(\epsilon)$ components of p_{11} and r_{11}. Furthermore, one can in a similar way find asymptotic approximations of p_{3k}, r_{3k} and p_{1n}, r_{1n} which all are of the order of $O(\epsilon)$. This procedure is described in detail by Faltinsen *et al.* (2003) for sloshing in a three-dimensional rectangular tank. Specifically, we arrive at the $\bar\sigma_{0k}^2-4$ and $\bar\sigma_{2k}^2-4$ denominators in expressions (4.9) and denominators $(\sigma_{3k}/\sigma)^2-9=\bar\sigma_{3k}^2-9$ and $(\sigma_{1k}/\sigma)^2-9=\bar\sigma_{1n}^2-9$ will appear in expressions for p_{3k}, r_{3k} and p_{1n}, r_{1n}, respectively. The denominators can be close to zero for certain forcing frequencies in the primary resonance zone $\sigma/\sigma_{11}\approx 1$. This makes the constructed asymptotic steady-state solution invalid and indicates occurrence of secondary resonance which leads to failure of the Moiseev–Narimanov modal equations unless the forcing amplitude is very small so that nonlinear transfer of energy between modes asymptotically disappears. The secondary resonance phenomenon within the framework of the Moiseev–Narimanov asymptotics implies that at least one of the conditions

$$2\sigma\approx\sigma_{0i},\quad 2\sigma\approx\sigma_{2i},\quad 3\sigma\approx\sigma_{3i}\quad\text{or}\quad 3\sigma\approx\sigma_{1(i+1)}\quad(i\geqslant 1) \tag{4.13}$$

is satisfied in a neighbourhood of the primary resonance zone $\sigma\approx\sigma_{11}$. When introducing

$$i_{mi}(h)=\frac12\sqrt{\frac{\kappa_{mi}}{\kappa_{11}}},\quad m=0,2;\qquad i_{mi}(h)=\frac13\sqrt{\frac{\kappa_{mi}}{\kappa_{11}}},\quad m=1,3;\ i\geqslant 1, \tag{4.14}$$

https://doi.org/10.1017/jfm.2012.635 Published online by Cambridge University Press

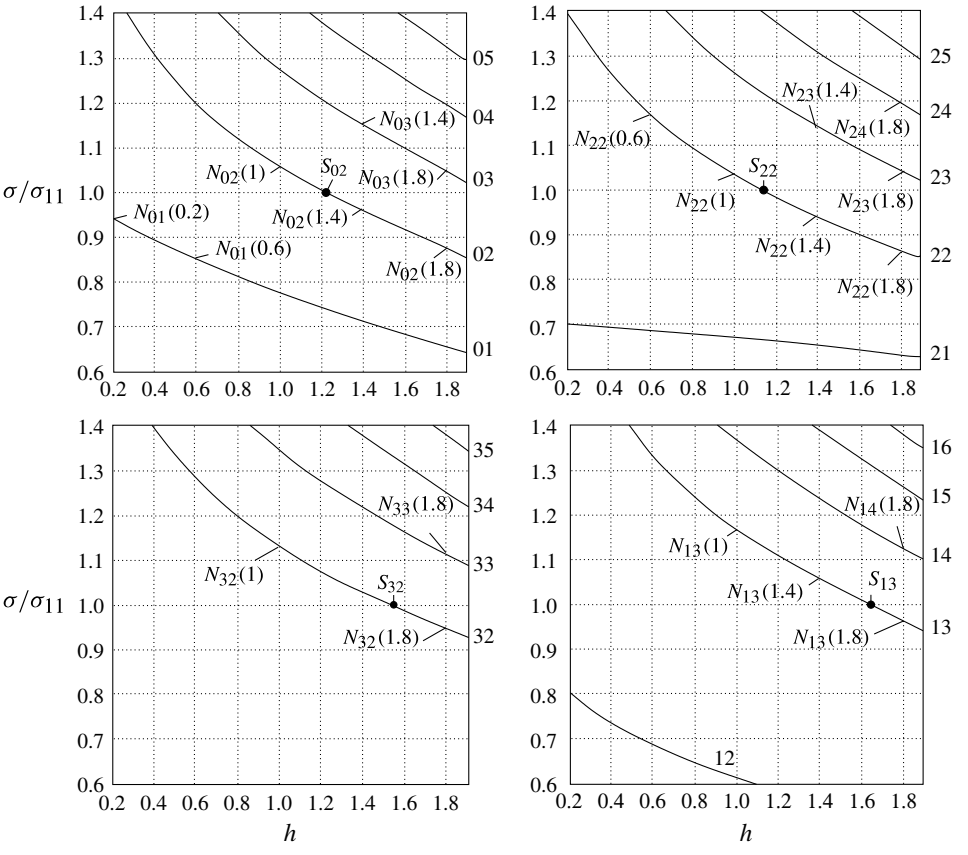


FIGURE 3. Graphic estimates of secondary resonances for steady-state sloshing within the framework of the Moiseev–Narimanov asymptotics. Points $N_{Mi}(h) = (h, i_{Mi}(h))$ on the (Mi) graphs are functions of the non-dimensional depth h where i_{Mi} are computed by (4.14) and imply σ/σ_{11} for which a secondary resonance with respect to the (Mi) mode occurs. Because the Moiseev–Narimanov asymptotics postulates the primary resonance condition $\sigma \to \sigma_{11}$, secondary resonance is not avoidable at the critical liquid depths $h_{02} = 1.219\ldots$, $h_{22} = 1.129\ldots$, $h_{32} = 1.529\ldots$ and $h_{13} = 1.642\ldots$ (denoted by the points S_{02}, S_{22}, S_{32} and S_{13}). The graphs can closely approach to the primary resonance zone for $1.0 \lesssim h \leqslant 1.9$ exemplified by points $N_{Mi}(h)$ at $h = 0.2$, 1.0, 1.4 and 1.8 corresponding to experiments by Sumner & Stofan (1963).

these conditions read as '$\sigma/\sigma_{11} \approx i_{mi}(h)$ for at least one pair (mi), $m = 0, 1, 2, 3$; $i \geqslant 1$ as $\sigma/\sigma_{11} \approx 1$'.

Figure 3 presents the graphs $i_{mi}(h)$ and thereby gives a graphic estimate of the secondary resonance. The secondary resonance is unavoidable when $\sigma/\sigma_{11} = 1$ and $\sigma/\sigma_{11} = i_{mi}$ for a certain pair (mi). This case is denoted by points S_{02}, S_{22}, S_{32} and S_{13} for the critical liquid depths $h_{02} = 1.219\ldots$, $h_{22} = 1.129\ldots$, $h_{32} = 1.529\ldots$ and $h_{13} = 1.642\ldots$, respectively. As long as h is close to these critical depths, the Moiseev–Narimanov asymptotic theories (including (4.2)–(4.5)) are not applicable.

When one of the denominators $\bar{\sigma}_{0k}^2 - 4$, $\bar{\sigma}_{0k}^2 - 4$, $\bar{\sigma}_{3k}^2 - 9$ or $\bar{\sigma}_{1n}^2 - 9$ is less than $O(\epsilon^{1/3})$, the asymptotic steady-state solution with respect to the small parameter $\epsilon^{1/3}$ is invalid. Adopting the so-called Moiseev asymptotic detuning $\delta = (\bar{\sigma}_{11}^2 - 1) = O(\epsilon^{2/3})$

https://doi.org/10.1017/jfm.2012.635 Published online by Cambridge University Press

proposed by Moiseev (1958) to ensure the quantities in (4.10) are of the same order, the failure implies that a secondary resonance is possible when $|i_{mi}(h) - 1| \lesssim O(\epsilon^{1/3})$ for a certain pair mi ($m = 0, \ldots, 3$ and $i \geqslant 1$) in the primary resonance range $-O(\epsilon^{2/3}) \lesssim \sigma/\sigma_{11} - 1 \lesssim O(\epsilon^{2/3})$. When taking, for instance, the mean non-dimensional experimental forcing amplitude $\epsilon = 0.008$ from experiments by Sumner & Stofan (1963), we can estimate the possibility of the secondary resonance as $|i_{mi}(h) - 1| \lesssim 0.2$. This is a quite broad zone and many secondary resonances become theoretically possible (but not necessarily occurring) for this forcing amplitude as marked by points N_{mi} in figure 3. The secondary resonance is more dangerous when it occurs for the second-order modes p_{0k}, p_{2k} and r_{2k}. This is associated with N_{0k} and N_{2k} in figure 3. Probability of the secondary resonance is higher for higher liquid depths, $1 \lesssim h \leqslant 1.9$. An adaptive multimodal ordering will be needed to handle the secondary resonances as in Faltinsen *et al.* (2006) for three-dimensional rectangular tank shape.

Assuming that there are no secondary resonances so that the aforementioned denominators are of the order $O(1)$ on the $\epsilon^{1/3}$ scale, we consider $m_1(\bar{\sigma}_{11}^2) = O(1)$ and $m_3(\bar{\sigma}_{11}^2) = O(1)$ in (4.10) and expand them in Taylor series by the Moiseev detuning $\delta = (\bar{\sigma}_{11}^2 - 1)$. Substituting this expansion in (4.10) and excluding the $o(\epsilon)$-order terms replaces m_1 and m_3 by $m_1^{(0)} = m_1(1)$ and $m_3^{(0)} = m_3(1)$, respectively. The coefficients $m_1^{(0)}$ and $m_3^{(0)}$ remain being functions of h.

As shown by Faltinsen *et al.* (2003) and Gavrilyuk *et al.* (2007), the solvability condition of (4.10) requires $\bar{A} = \bar{B} = 0$ and, the system has only two different solutions. The first solution implies *planar* steady-state waves with $B = 0$ for which the only non-zero dominant amplitude A is governed by

$$A\left[(\bar{\sigma}_{11}^2 - 1) + m_1^{(0)}A^2\right] = e_1\eta_{1a}. \tag{4.15}$$

The second solution implies *swirling* whose two non-zero dominant amplitude parameters A and B are the roots of the system

$$\begin{cases} A\left[(\bar{\sigma}_{11}^2 - 1) + (m_1^{(0)} + m_3^{(0)})A^2\right] = -\dfrac{m_1^{(0)}}{m_1^{(0)} - m_3^{(0)}}e_1\eta_{1a}, \\ B^2 = -\dfrac{(\bar{\sigma}_{11}^2 - 1) + m_3^{(0)}A^2}{m_1^{(0)}} > 0. \end{cases} \tag{4.16}$$

Chapter 9 of Faltinsen & Timokha (2009) gives details on the asymptotic stability analysis based on the dominant amplitude parameters in (4.10). The steady-state solution is unstable when the eigenvalues of the 4×4 matrix C with non-zero elements

$$c_{12} = -[\bar{\sigma}_1^2 - 1 + m_1^{(0)}A^2 + m_1^{(0)}B^2]; \quad c_{21} = \bar{\sigma}_1^2 - 1 + 3m_1^{(0)}A^2 + m_3^{(0)}B^2,$$
$$c_{14} = -(m_1^{(0)} - m_3^{(0)})AB; \quad c_{41} = -2m_3^{(0)}AB; \quad c_{23} = 2ABm_3^{(0)}; \quad c_{32} = (m_1^{(0)} - m_3^{(0)})AB,$$
$$c_{34} = \bar{\sigma}_1^2 - 1 + m_1^{(0)}B^2 + m_1^{(0)}A^2; \quad c_{43} = -[\bar{\sigma}_1^2 - 1 + 3m_1^{(0)}B^2 + m_3^{(0)}A^2]$$

have a non-zero positive real part. In terms of the characteristic polynomial of the matrix, $\lambda^4 + c_1\lambda^2 + c_0 = 0$, the stability requires $c_0 > 0$, $c_1 > 0$ and $c_1^2 - 4c_0 > 0$.

4.4. *Response curves and stability boundaries*

For $0 < h \lesssim 1$, the amplitude parameters A and B constitute the three-dimensional response curves plotted in figure 4(*a*). The response curves were computed and drawn for $h = 0.6$ and $(\epsilon/2)^{2/3} = 0.03$ ($\epsilon = \eta_{1a} = 0.0104$) which correspond to an

https://doi.org/10.1017/jfm.2012.635 Published online by Cambridge University Press

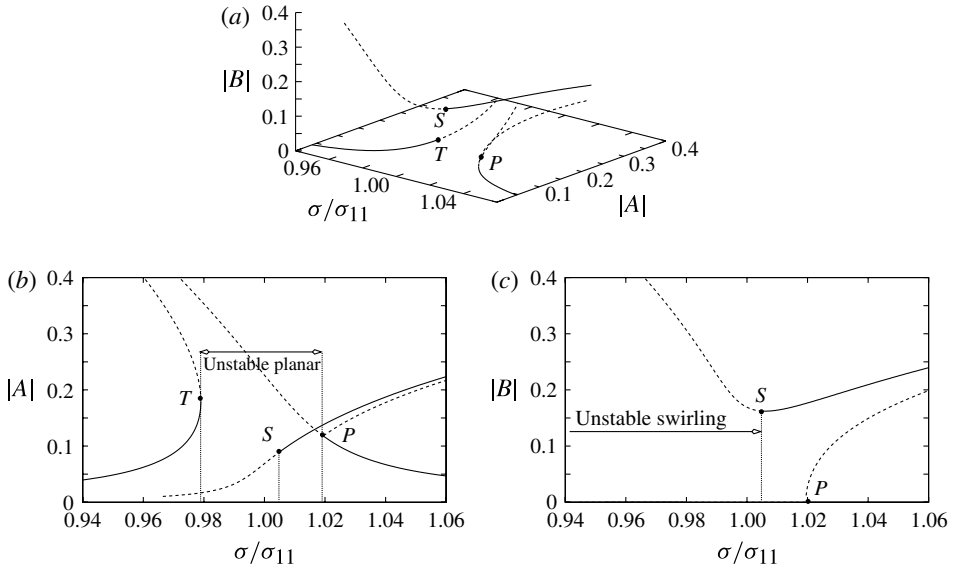


FIGURE 4. Three-dimensional response curves in the $(\sigma/\sigma_{11}, |A|, |B|)$ space (a) and their projections on the $(\sigma/\sigma_{11}, |A|)$ and $(\sigma/\sigma_{11}, |B|)$ planes (b,c) that are typical for $0 < h \lesssim 1$. Computations are done with $h = 0.6$ and $(\epsilon/2)^{2/3} = 0.03$ ($\epsilon = \eta_{1a} = 0.0104$). Solid lines denote stable solutions, but dashed lines imply unstable steady-state waves. The abscissas of T and P, σ_T/σ_{11} and σ_P/σ_{11}, respectively, determine the primary resonance region where planar waves are unstable, but point S (abscissa σ_S/σ_{11}) denotes Hopf bifurcation where swirling becomes unstable with decreasing the forcing frequency. The frequency range between σ_T/σ_{11} and σ_S/σ_{11} implies there are no stable steady-state wave regimes and, therefore, irregular waves occur.

experimental case by Sumner & Stofan (1963) and Sumner (1966). The response curves lying in the $(\sigma/\sigma_{11}, |A|)$ plane ($B = 0$) correspond to planar steady-state waves, but the three-dimensional curves with $B \neq 0$ imply swirling. Solid lines denote stable time-periodic solutions but dashed lines mark unstable ones. In addition to the three-dimensional view, we present projections of the response curves on the $(\sigma/\sigma_{11}, |A|)$ and $(\sigma/\sigma_{11}, |B|)$ planes (in figure 4*b,c*).

As was remarked in the previous section, the response curves should be qualitatively identical to those established for the circular-base tank (Gavrilyuk *et al.* 2000, 2007) and differences are only associated with actual positions of the three bifurcation points denoted by T (turning point), P (Poincaré bifurcation) and S (Hopf bifurcation). Similar to the circle-base tank case (see, e.g., Miles 1984*a*,*b*; Gavrilyuk *et al.* 2000, 2007), abscissas of these bifurcation points determine the stability boundaries of the steady-state regimes: (i) σ_T/σ_{11} defines the stability boundary between stable planar waves with $\sigma/\sigma_{11} < \sigma_T/\sigma_{11}$ and irregular waves expected between abscissas of T and S; (ii) σ_S/σ_{11} is the stability boundary between irregular waves for $\sigma_T/\sigma_{11} < \sigma/\sigma_{11} < \sigma_S/\sigma_{11}$ and stable swirling in the range $\sigma_S/\sigma_{11} < \sigma/\sigma_{11} < \sigma_P/\sigma_{11}$; and (iii) σ_P/σ_{11} is the stability boundary between the stable swirling region and the frequency range $\sigma_P/\sigma_{11} < \sigma/\sigma_{11}$ in which both swirling and planar waves are stable. Theoretically, the stability boundaries associated with T, S and P are functions of h and the forcing amplitude ϵ.

https://doi.org/10.1017/jfm.2012.635 Published online by Cambridge University Press

4.5. *Comparison with experiments*

Sumner & Stofan (1963) conducted a series of model tests to estimate the stability boundaries T, S and P. The tests were conducted over a wide range of excitation amplitudes in tanks with diameters of 0.813, 0.523 and 0.241 m. The liquid was water in all cases. The tanks were fabricated from clear plastic. The highest excitation amplitude is $0.029R_0$ that is clearly smaller than the largest possible amplitude for ships. Because the model tank dimensions are relatively small, one can employ the Bond number $\mathrm{Bo} = gd_l^2\rho/T_s$, where d_l is the mean free surface diameter, ρ is the liquid density and T_s is the surface tension coefficient, to examine whether the surface tension matters for the global wave behaviour. The value of T_s for the air–water interface at 20 °C is equal to 0.073 N m^{-1}. The lowest possible Bond number Bo expected for the lowest tank radius and the depth-to-radius ratios 0.2 and 1.8 is equal to 2816. As was discussed by Faltinsen & Timokha (2009, pp. 124–125), the surface tension effect on the global wave behaviour can be neglected in the dynamic boundary conditions for $100 \lesssim \mathrm{Bo}$, but the capillary meniscus continues influencing near-wall elevations as $\mathrm{Bo} \lesssim 10^4$. This means that our mathematical model is applicable for the experimental cases to validate the constructed time-periodic solutions, but one should, generally, include a meniscus effect for comparing theoretical and experimental wave elevations at the tank wall. Five different tank fillings were tested associated with non-dimensional depths 0.2, 0.6, 1.0, 1.4 and 1.8. The interested reader can find more on equipment and model test details in the original report which is freely available online at the NASA report database.

Before starting a comparison of our theoretical stability boundaries with those following from experiments by Sumner & Stofan (1963), we should remark that the report normally does not give the stability boundaries but rather their bounds. It is a consequence of the forcing-frequency stepping in the experimental series. After setting a constant forcing amplitude, Sumner & Stofan (1963) did initially set the forcing frequency well below or above the first fundamental sloshing frequency ensuring that the stable planar wave regime was established. The forcing frequency was then varied in small discrete increments to approach the first natural sloshing frequency. In the forthcoming graphic representations, empty symbols were used to denote the last stable steady-state sloshing (planar or swirling), but filled symbols mark the closest frequency to the empty-symbol forcing frequency where planar or swirling become unstable due to an increase/decrease of the forcing frequency. Normally, the two empty–solid symbols come in pairs and the actual stability boundary is expected somewhere between them. This is depicted in figures 5 and 6 where symbols △ and ▲ are for $R_0 = 0.1205$ m, ◇ and ◆ correspond to $R_0 = 0.2615$ m and ○ and ● are associated with $R_0 = 0.4065$ m. The figures give a comparison for $h = 0.2$, 0.6 and 1.0 with original notation and normalizations by Sumner & Stofan (1963). Because T is situated below the primary resonance where the frequency increments were positive, the empty symbols denote a lower bound of the stability boundary but the solid symbols imply an upper bound. It is opposite for S and P (except one experimental point for S with $h = 0.6$) for which the forcing-frequency stepping was negative.

The case $h = 0.2$ is considered in figure 5(*a*) which shows that the stability boundaries P and S are well predicted but there is a discrepancy for T. Reporting on the forcing frequencies about T, Sumner & Stofan (1963) detected a '…region lying roughly parallel to but displaced slightly from the lower stability boundary in the stable planar region where a vertical (axisymmetric) oscillations of the liquid at the vertical axis of symmetry of the tank appeared and was superimposed on the normal planar (asymmetric) motion of the liquid surface. The frequency of this vertical

https://doi.org/10.1017/jfm.2012.635 Published online by Cambridge University Press

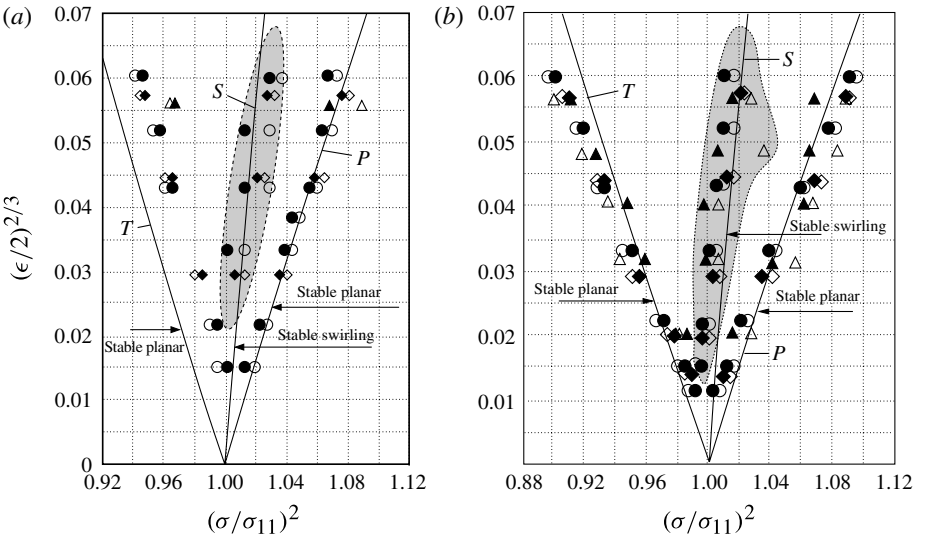


FIGURE 5. Experimental estimates and theoretical predictions of stability boundaries T, S and P versus forcing amplitude $\epsilon = \eta_{1a}$ for $h = 0.2$ (a) and $h = 0.6$ (b). Empty (stable) and solid (unstable) symbols denote experimental bounds of the experimental stability boundaries by Sumner & Stofan (1963). The symbols related to the stability boundary S are covered by a shadow area. The symbols correspond to experiments made for the three different tank radii: (△ and ▲) $R_0 = 0.1205$ m; (◇ and ◆) $R_0 = 0.2615$ m; and (○ and ●) $R_0 = 0.4065$ m. The theoretical stability boundaries are marked by T, P and S that corresponds σ_T/σ_{11}, σ_S/σ_{11} and σ_P/σ_{11}, respectively, versus $(\epsilon/2)^2$. A discrepancy for T in (a) can be explained by the secondary resonance with respect to the mode (01) estimated at $(\sigma/\sigma_{11})^2 = 0.892$ and confirmed in observations by Sumner & Stofan (1963) who discovered in this frequency region axisymmetric oscillations (superposed with antisymmetric ones) whose frequency is equal to twice the forcing frequency.

oscillation was equal to twice the excitation frequency…'. The appearance of the double forcing frequency with vertical free-surface motions indicates the secondary resonance with respect to an axisymmetric mode. Indeed, mode 01 is most likely resonantly amplified; its secondary resonance is evaluated at $(\sigma/\sigma_{11})^2 = 0.892$ (point $N_{01}(0.2)$ in figure 3).

Theory and experiments for $h = 0.6$ are compared in figure 5(b). For planar waves, the instability region is well predicted. A difference comes with increasing ϵ that can be explained by increasing the effective secondary resonance zone which starts covering $N_{01}(0.6)$ (influences T) and $N_{22}(0.6)$ (influences P). An indication is the fact that Sumner & Stofan (1963) reported the 2σ axisymmetric oscillations appearing slightly to the left of the stability boundary T for the larger forcing amplitudes.

Figure 6 presents theoretical and experimental results for the half-filled spherical tank ($h = 1.0$). We note an increase of the instability region for steady-state planar waves detected in experiments that is not described in full by our asymptotic theory. Figure 3 shows that secondary resonances are possible for $\sigma/\sigma_{11} > 1$ but we do not expect them for $\sigma/\sigma_{11} < 1$. In other words, the Moiseev–Narimanov theory should give a good prediction for T but not necessarily for S and P. As for T, the theoretical stability boundary is slightly beneath the experimental upper bound (solid symbols) but empty symbols (clearly stable planar waves) are separated for larger forcing

https://doi.org/10.1017/jfm.2012.635 Published online by Cambridge University Press

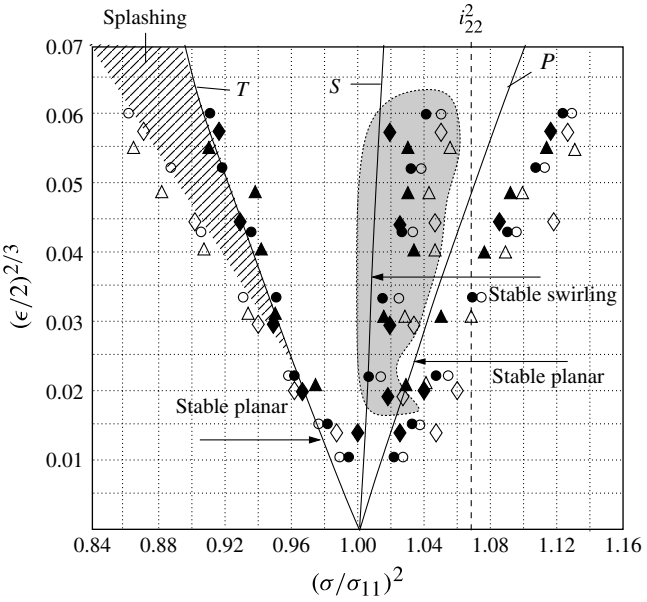


FIGURE 6. The same as in figure 5 but for $h = 1.0$. A novelty is the experimental 'splashing' zone that introduces a difference between empty (clearly stable planar waves) and solid (clearly irregular waves) symbols. Sumner & Stofan (1963) introduced the 'splashing' zone to report on near-wall overturning waves causing free-surface fragmentation (without a rotary component). Theoretical T coincides with the upper experimental bound. A discrepancy for S and P can be explained by the secondary resonance zone at $(\sigma/\sigma_{11})^2 = i_{22}^2 = 1.0671\ldots$ ($N_{22}(1.0)$ in figure 4) leading to resonant amplification of mode 22.

amplitudes by a new region 'splashing' introduced by Sumner & Stofan (1963). Describing sloshing in this region, Sumner & Stofan (1963) write that 'no rotation of the nodal diameter was observed in this splash region' but 'drops splashed from the tank wall and showered through the ullage', i.e. they describe overturning waves at the tank surface accompanied by a free-surface fragmentation. In our opinion, Sumner & Stofan (1963) incorrectly related this phenomenon to a kind of instability. Instability of planar waves should lead to three-dimensional wave patterns (most likely rotary motions) which are not observed in experiments. We have therefore re-classified 'splashing' as stable steady-state planar waves that, due to the curvilinear wall, cause local near-wall phenomena becoming stronger with increasing amplitude. However, there is a discrepancy between theoretical and experimental S and P. It is clarified by the secondary resonance phenomenon. The most dangerous secondary resonance occurs at $(\sigma/\sigma_{11})^2 = i_{22}^2 = 1.0671\ldots$ ($N_{22}(1.0)$ in figure 4), i.e. exactly in the middle of the experimental forcing frequency range in the right of $\sigma/\sigma_{11} = 1$. The Moiseev–Narimanov theory is invalid around $\sigma/\sigma_{11} = i_{22}$.

Sumner & Stofan (1963) also reported experimental results for $h = 1.4$ and 1.8. Our attempt to find a consistency between our asymptotic prediction and these experiments were unfortunately unsuccessful for all of the experimental forcing amplitudes due to unrealistically large $\cos(2\sigma t)$ and $\sin(2\sigma t)$ components in (4.8) caused by increase of the c_{12} and s_{12} coefficients by (4.9). This means that p_{22}, r_{22} and p_{02} become of the same dominant order as p_{11} and r_{11} and, therefore, the Moiseev–Narimanov asymptotics is questionable for these two experimental

https://doi.org/10.1017/jfm.2012.635 Published online by Cambridge University Press

cases. The failure of the Moiseev–Narimanov modal system is explained by the secondary resonance phenomena. For $h = 1.4$, it is estimated at $(\sigma/\sigma_{11})^2 = i_{02}^2 = 0.918$, $i_{22}^2 = 0.8841$, $i_{32}^2 = 1.0563$ and $i_{13}^2 = 1.116$ which belong to the experimental frequency range $0.75 < (\sigma/\sigma_{11})^2 < 1.3$ where strongly nonlinear sloshing was observed. For $h = 1.8$, the experimental frequency range is broader, $0.6 < (\sigma/\sigma_{11})^2 < 1.5$ and one should expect multiple secondary resonances marked by $N_{mi}(1.8)$ in figure 3. Finally, one should also note that these experimental cases are characterized by a sufficient increase of the 'splashing' zone, especially for $h = 1.8$ where overturning waves occur almost always in the experimental frequency range.

5. Conclusions

The present paper is a first attempt to construct an analytical sloshing theory of nonlinear sloshing in a spherical tank and explain famous experimental results by Sumner & Stofan (1963). Under certain circumstances, the paper can be interpreted as a generalization of theoretical results by Faltinsen *et al.* (2003) on resonant liquid sloshing in a square-base tank. Two classes of theoretical results are reported. First, we generalize the multimodal method for the spherical geometry. Second, because the modal methods are currently a unique existing analytical approach to study the steady-state (time-periodic) three-dimensional wave regimes occurring due to horizontal harmonic excitations of the lowest natural sloshing frequency (see Miles (1984*a*,*b*), Gavrilyuk *et al.* (2000, 2007) and Faltinsen *et al.* (2003) and references therein), we employed the derived Moiseev–Narimanov modal system for theoretical classification of these wave regimes.

The generalization of the multimodal method became possible by using the analytically approximate natural sloshing modes by Faltinsen & Timokha (2012) and curvilinear spatial coordinates (the so-called non-conformal mapping technique) by Lukovsky (1975). Three systems of nonlinear modal equations were derived, namely: (i) fully nonlinear modal equations coupling the generalized coordinates and velocities (equations (3.10) and (3.11)) which were early known only for liquid sloshing in tanks with upright walls at the free surface; (ii) weakly nonlinear modal equations (3.19) with respect to the generalized coordinates keeping the third-order polynomial quantities (generalization of the Faltinsen *et al.* 2003, results for square-base tank); (iii) the Moiseev–Narimanov asymptotic modal equations (equations (4.2)–(4.5)) which are a generalization of analogous modal equations for upright rectangle- and circle-base tanks by Faltinsen *et al.* (2003), Lukovsky *et al.* (2012) and Takahara & Kimura (2012). These three types of nonlinear modal equations already exist for the case of a square-base tank (Faltinsen *et al.* 2003). Computational formulas for (ii) and (iii) are presented in appendices A and B. They appear more complicated than those for a square-base tank but remain the same from an algorithmic point of view; similar notation is kept. As Love & Tait (2010, 2011), Takahara & Kimura (2012) and Takahara *et al.* (2012) showed for the square-base case, the formulas may be adopted and repeated by other researchers working on appropriate engineering applications. A numerical difficulty can only be that the formulas for spherical tank involve analytically approximate natural modes by Faltinsen & Timokha (2012). Other researchers have to repeat results on the natural sloshing modes or, alternatively, propose other analytically approximate methods to get the natural sloshing modes which possess desirable features. Supplementary materials available at http://dx.doi.org/10.1017/jfm.2012.635 with tables of hydrodynamic coefficients in

https://doi.org/10.1017/jfm.2012.635 Published online by Cambridge University Press

the Moiseev–Narimanov modal equations should help other researchers to control their computational results.

The three systems (i), (ii) and (iii) play different roles in our analysis. The system (i) is of the auxiliary character. The weakly nonlinear modal equations (ii) can be considered as a basis for the Moiseev–Narimanov and diverse adaptive asymptotic modal systems. Bearing in mind the similarity of (ii) and (iii) and their analogies for the square-base tank obtained by Faltinsen *et al.* (2003), it is expected that the Moiseev–Narimanov asymptotic modal system should provide an accurate theoretical prediction of the steady-state (time-periodic) resonant wave regimes occurring due to harmonic excitation of the lowest natural frequency with relatively small forcing amplitude, their stability boundaries (the so-called theoretical classification; Faltinsen *et al.* 2005*a*), but the adaptive modal systems following from (ii) will be required to obtain a precise quantitative agreement with experiments on wave response (wave elevation, hydrodynamic force and moment) for transient and time-periodic waves. The adaptive modal systems are especially important when the forcing amplitude increases and/or the secondary resonances occur. For a square-base tank, the first task (classification of steady-state resonant wave regimes) was solved by Faltinsen *et al.* (2003, 2005*a*), but the corresponding adaptive modal systems were analysed by Faltinsen *et al.* (2005*b*) and Faltinsen *et al.* (2006).

The famous NASA reports by Sumner & Stofan (1963) and Sumner (1966) present experimental results on classification of the steady-state wave regimes for spherical tanks. Up to now, these results were not explained theoretically from a hydrodynamical point of view (Sumner & Stofan (1963) used a pendulum analogy introducing the planar, swirling and irregular wave motions). The present paper uses the Moiseev–Narimanov asymptotic modal system for such a theoretical prediction of the steady-state wave regimes and the stability boundaries between them. As we pointed out, this is a generalization of theoretical results by Faltinsen *et al.* (2003, 2005*a*) to the spherical tank shape. Planar and swirling (rotary) steady-state wave regimes are detected that is consistent with the experimental observations by Sumner & Stofan (1963) as well as analogous results for an upright circular cylindrical tank by Miles (1984*a*,*b*) and Gavrilyuk *et al.* (2000, 2007). Moreover, the secular equations with respect to the dominant amplitude parameters have the same structure as those in Gavrilyuk *et al.* (2000, 2007). This implies qualitatively similar response curves and bifurcation points. Stability analysis establishes frequency regions where these steady-state motions are stable and identifies stability boundaries of these regions as well as a frequency range where both regimes are unstable and irregular sloshing occurs. Theoretical results on the stability boundaries are validated by experimental results of Sumner & Stofan (1963). The theory and experiments are in a good agreement for the liquid depth-to-radius ratios $0.2 \lesssim h \lesssim 1$ when the secondary resonance phenomena is of minor importance and local breaking with overturning waves called 'splashing' by Sumner & Stofan (1963) appear only in rather narrow frequency ranges. The possibility of secondary resonances and 'splashing' dramatically increases for the larger liquid depths $1 \lesssim h < 2$.

The four critical liquid depth-to-radius ratios $h = 1.129\ldots$, $1.219\ldots$, $1.529\ldots$ and $1.642\ldots$ were found. Secondary resonance leads to amplification of double and triple harmonics in higher modes at the critical depths which may make the Moiseev–Narimanov modal system invalid. Based on the results by Faltinsen *et al.* (2005*b*, 2006), one can expect that accounting for the secondary resonance matters for quantification of the wave response (free-surface elevation, hydrodynamic force and moment), in particular, in transient conditions and with increasing the forcing magnitude. This means that both analysing the resonant liquid sloshing for the larger

https://doi.org/10.1017/jfm.2012.635 Published online by Cambridge University Press

depths, $1 \lesssim h < 2$, and quantification of the wave responses can need an adaptive multimodal system as in Faltinsen *et al.* (2005*b*, 2006) for square-base tanks. Such a modal system should be our forthcoming task. A difficulty is that quantitative experimental results on the wave response are rare and, perhaps, limited to a few measurements of the hydrodynamic force by Stofan & Armsted (1962) and Hysing (1976). Stofan & Armsted (1962)' experiments were performed for relatively small forcing amplitudes, and therefore can be well described within the framework of linear sloshing theory. The measurements by Hysing (1976) were done with relatively large forcing amplitudes when a strong splashing occurs. An alternative method of validation could be dedicated CFD calculations performed for some input parameters.

Supplementary data

Supplementary data are available at http://dx.doi.org/10.1017/jfm.2012.635.

Appendix A. Basic formulas

The wave patterns in axisymmetric tanks, in general, and in a spherical tank, in particular, are characterized by sin and cos behaviour in the angular direction, but, in the radial direction, the wave patterns are defined by projections of the natural sloshing modes on the mean free surface $f^*_{mi}(r_*) = \phi^*_{mi}(r_*, z_0)$ and their derivatives with respect to r_*.

For the angular direction, we involve the tensor-type coefficient

$$\Lambda_{\underbrace{i\ldots j}_{N_1}\underbrace{n\ldots k}_{N_2}} = \int_{-\pi}^{\pi} \underbrace{\cos(i\theta)\ldots\cos(j\theta)}_{N_1} \cdot \underbrace{\sin(n\theta)\ldots\sin(k\theta)}_{N_2}\, \mathrm{d}\theta \tag{A 1}$$

which can be computed analytically by a recursive formula starting with the case $N_1 + N_2 = 2$. For the radial direction, we consider $f^*_{mi}(r_*)$ and define

$$f_{\alpha\beta}(r) = \phi^*_{\alpha,\beta}(rr_0, z_0); \quad f^r_{\alpha\beta}(r) = \frac{\partial\phi^*}{\partial r_*}(rr_0, z_0); \quad f^{rr}_{\alpha\beta}(r) = \frac{\partial^2\phi^*}{\partial r_*^2}(rr_0, z_0) \tag{A 2}$$

which can be found from the analytical approximate solution by Faltinsen & Timokha (2012). A series of tensor-type coefficients is

$$\lambda_{(mi)\ldots(nj)} = \int_0^1 r f_{mi}\ldots f_{nj}\, \mathrm{d}r. \tag{A 3}$$

A.1. *Integrals A^p_{Mi} and A^r_{mi} defined by (3.12)*

Expanding A^p_{Mi} and A^r_{mi} up to the third polynomial order in p_{Mi} and r_{mi} gives

$$A^p_{Ab} = \text{const} + r_0^3\Lambda_{AA}p_{Ab} + \frac{1}{2}\sum_{MNij}\chi^{pp}_{(Mi)(Nj),(Ab)}\,p_{Mi}p_{Nj} + \frac{1}{2}\sum_{mnij}\chi^{rr}_{(mi)(nj),(Ab)}\,r_{mi}r_{nj}$$
$$+ \frac{1}{3}\sum_{MNKijl}\chi^{ppp}_{(Mi)(Nj)(Kl),(Ab)}\,p_{Mi}p_{Nj}p_{Kl} + \sum_{Mnkijl}\chi^{prr}_{(Mi),(nj)(kl),(Ab)}\,p_{Mi}r_{nj}r_{kl}, \tag{A 4a}$$

$$A^r_{ab} = \text{const} + r_0^3\Lambda_{aa}r_{ab} + \sum_{Mnij}\chi^{pr}_{(Mi),(nj),(ab)}\,p_{Mi}r_{nj} + \frac{1}{3}\sum_{mnkijl}\chi^{rrr}_{(mi)(nj)(kl),(ab)}\,r_{mi}r_{nj}r_{kl}$$
$$+ \sum_{MNkijl}\chi^{ppr}_{(Mi)(Nj),(kl),(ab)}\,p_{Mi}p_{Nj}r_{kl}; \tag{A 4b}$$

https://doi.org/10.1017/jfm.2012.635 Published online by Cambridge University Press

so that

$$\frac{\partial A^{p}_{Ab}}{\partial p_{Df}} = r_0^3 \Lambda_{AD}\delta_{bf} + \sum_{Mi} \chi^{pp}_{(Mi)(Df),(Ab)} p_{Mi} + \sum_{NKjl} \chi^{ppp}_{(Df)(Nj)(Kl),(Ab)} p_{Nj} p_{Kl} + \sum_{nkjl} \chi^{prr}_{(Df),(nj)(kl),(Ab)} r_{nj} r_{kl}, \tag{A 5a}$$

$$\frac{\partial A^{p}_{Ab}}{\partial r_{df}} = \sum_{mi} \chi^{rr}_{(mi)(df),(Ab)} r_{mi} + 2\sum_{Mnij} \chi^{prr}_{(Mi),(nj)(df),(Ab)} p_{Mi} r_{nj}, \tag{A 5b}$$

$$\frac{\partial A^{r}_{ab}}{\partial p_{Df}} = \sum_{nj} \chi^{pr}_{(Df),(nj),(ab)} r_{nj} + 2\sum_{Mnij} \chi^{ppr}_{(Mi)(Df),(nj),(ab)} p_{Mi} r_{nj}, \tag{A 5c}$$

$$\frac{\partial A^{r}_{ab}}{\partial r_{df}} = r_0^3 \Lambda_{ad}\delta_{bf} + \sum_{Mi} \chi^{pr}_{(Mi),(df),(ab)} p_{Mi} + \sum_{mnij} \chi^{rrr}_{(mi)(nj)(df),(ab)} r_{mi} r_{nj} + \sum_{MNij} \chi^{ppr}_{(Mi)(Nj),(df),(ab)} p_{Mi} p_{Nj}. \tag{A 5d}$$

Here,

$$\chi^{pp}_{(Mi)(Nj),(Ab)} = r_0^2 \Lambda_{AMN,}\, \lambda^{(1)}_{(Mi)(Nj),(Ab)}; \quad \chi^{rr}_{(mi)(nj),(Ab)} = r_0^2 \Lambda_{A,mn} \lambda^{(1)}_{(mi)(nj),(Ab)},$$

$$\chi^{ppp}_{(Mi)(Nj)(Kl),(Ab)} = r_0^3 \Lambda_{MNKA,}\, \lambda^{(2)}_{(Mi)(Nj)(Kl),(Ab)} + \frac{r_0 z_0}{\pi}\left(\Lambda_{MA}\lambda^{(1)}_{(Ai),(Ab)}\Lambda_{NK}\delta_{jl} + \Lambda_{KA}\lambda^{(1)}_{(Al),(Ab)}\Lambda_{MN}\delta_{ij} + \Lambda_{NA}\lambda^{(1)}_{(Aj),(Ab)}\Lambda_{MK}\delta_{il}\right),$$

$$\chi^{prr}_{(Mi),(nj)(kl),(Ab)} = r_0^3 \Lambda_{MA,nk}\lambda^{(2)}_{(Mi)(nj)(kl),(Ab)} + r_0 z_0 \Lambda_{MA}\lambda^{(1)}_{(Ai),(Ab)}\delta_{nk}\delta_{jl},$$

$$\chi^{rrr}_{(mi)(nj)(kl),(ab)} = r_0^3 \Lambda_{,mnka}\lambda^{(2)}_{(mi)(nj)(kl),(ab)} + r_0 z_0 \left(\Lambda_{ma}\lambda^{(1)}_{(ai),(ab)}\delta_{kn}\delta_{jl} + \Lambda_{na}\lambda^{(1)}_{(aj),(ab)}\delta_{mk}\delta_{il} + \Lambda_{ka}\lambda^{(1)}_{(al),(ab)}\delta_{mn}\delta_{ij}\right);$$

$$\chi^{pr}_{(Mi),(nj),(ab)} = r_0^2 \Lambda_{M,na}\lambda^{(1)}_{(Mi)(nj),(ab)},$$

$$\chi^{ppr}_{(Mi)(Nj),(kl),(ab)} = r_0^3 \Lambda_{MN,ka}\lambda^{(2)}_{(Mi)(Nj)(kl),(ab)} + \frac{r_0 z_0}{\pi}\Lambda_{ka}\lambda^{(1)}_{(al),(ab)}\Lambda_{MN}\delta_{ij},$$

where

$$\lambda^{(1)}_{(mi)\ldots(nj),(\alpha\beta)} = \int_0^1 r f_{mi}\ldots f_{nj}\, F^{(1)}_{\alpha\beta}(r)\,\mathrm{d}r; \quad \lambda^{(2)}_{(mi)\ldots(nj),(\alpha\beta)} = \frac{1}{2}\int_0^1 r f_{mi}\ldots f_{nj}\, F^{(2)}_{\alpha\beta}(r)\,\mathrm{d}r,$$

within

$$F^{(2)}_{\alpha\beta}(r) = \left(\frac{\alpha^2}{r^2} - 2 - 4z_0\kappa_{\alpha\beta}\right) f_{\alpha\beta}(r) + \left(\frac{r^2(4z_0^2-1) - r_0^2}{r r_0} - (2z_0 r_0 \kappa_{\alpha\beta})r\right) f^{r}_{\alpha\beta}(r) + \left(z_0^2 r^2 - r_0^2\right) f^{rr}_{\alpha\beta}(r); \quad F^{(1)}_{\alpha\beta}(r) = (r_0^2\kappa_{\alpha\beta} - 2z_0) f_{\alpha\beta}(r) - (r_0 z_0)\, r f^{r}_{\alpha\beta}(r),$$

Even though there are $1/r$ quantities and functions $f^{rr}_{\alpha\beta}(r)$ are infinite due to the contact-line singularity within $(1-r)^{\gamma}$, $-1 < \gamma < 0$ (Lukovsky, Barnyak & Komarenko 1984), all the derived integrals are finite.

https://doi.org/10.1017/jfm.2012.635 Published online by Cambridge University Press

A.2. *Integrals* $A^{pp}_{(Mi)(Nj)}$, $A^{rr}_{(mi)(nj)}$ *and* $A^{pr}_{(Mi),(nj)}$ *defined by (3.13)*

Keeping the linear and quadratic terms in (3.13) gives

$$A^{pp}_{(Ab)(Cd)} = r_0^2 \Lambda_{AC}\delta_{bd}\kappa_{Ab} + \sum_{Mi} \Pi^{p,p}_{(Mi),(Ab)(Cd)} p_{Mi} + \sum_{MNij} \Pi^{p,pp}_{(Mi)(Nj),(Ab)(Cd)} p_{Mi}p_{Nj}$$
$$+ \sum_{mnij} \Pi^{p,rr}_{(mi)(nj),(Ab)(Cd)} r_{mi}r_{nj}; \quad A^{rr}_{(ab)(cd)} = r_0^2 \Lambda_{ac}\delta_{bd}\kappa_{ab} + \sum_{Mi} \Pi^{r,p}_{(Mi),(ab)(cd)} p_{Mi}$$
$$+ \sum_{MNij} \Pi^{r,pp}_{(Mi)(Nj),(ab)(cd)} p_{Mi}p_{Nj} + \sum_{mnij} \Pi^{r,rr}_{(mi)(nj),(ab)(cd)} r_{mi}r_{nj},$$
$$A^{pr}_{(Ab),(cd)} = \sum_{mi} \Pi^{r}_{(mi),(Ab),(cd)} r_{mi} + \sum_{Mnij} \Pi^{pr}_{(Mi),(nj),(Ab),(cd)} p_{Mi}r_{nj}. \tag{A 6}$$

Here,

$$\Pi^{p,p}_{(Mi),(Ab)(Cd)} = r_0 \left(\Lambda_{MAC,} K^{(0)}_{(Mi),(Ab)(Cd)} + \Lambda_{M,AC} L^{(0)}_{(Mi),(Ab)(Cd)} \right),$$
$$\Pi^{r,p}_{(Mi),(ab),(cd)} = r_0 \left(\Lambda_{M,ac} K^{(0)}_{(Mi),(ab)(cd)} + \Lambda_{Mac,} L^{(0)}_{(Mi),(ab)(cd)} \right),$$
$$\Pi^{p,pp}_{(Mi)(Nj),(Ab)(Cd)} = \frac{1}{2} r_0^2 \left(\Lambda_{MNAC,} K^{(1)}_{(Mi)(Nj),(Ab)(Cd)} + \Lambda_{MN,AC} L^{(1)}_{(Mi)(Nj),(Ab)(Cd)} \right)$$
$$+ \frac{z_0 \Lambda_{AC}\Lambda_{MN}\delta_{ij}}{\pi} \left(K^{(0)}_{,(Ab)(Cd)} + L^{(0)}_{,(Ab)(Cd)} \right),$$
$$\Pi^{p,rr}_{(mi)(nj),(Ab)(Cd)} = \frac{1}{2} r_0^2 \left(\Lambda_{AC,mn} K^{(1)}_{(mi)(nj),(Ab)(Cd)} + \Lambda_{,mnAC} L^{(1)}_{(mi)(nj),(Ab)(Cd)} \right)$$
$$+ z_0 \Lambda_{AC}\delta_{mn}\delta_{ij} \left(K^{(0)}_{,(Ab)(Cd)} + L^{(0)}_{,(Ab)(Cd)} \right),$$
$$\Pi^{r,pp}_{(Mi)(Nj),(ab)(cd)} = \frac{1}{2} r_0^2 \left(\Lambda_{MN,ac} K^{(1)}_{(Mi)(Nj),(ab)(cd)} + \Lambda_{MNac,} L^{(1)}_{(Mi)(Nj),(ab)(cd)} \right)$$
$$+ \frac{z_0}{\pi} \Lambda_{MN}\delta_{ij}\Lambda_{ac} \left(K^{(0)}_{,(ab)(cd)} + L^{(0)}_{,(ab)(cd)} \right),$$
$$\Pi^{r,rr}_{(mi)(nj),(ab)(cd)} = \frac{1}{2} r_0^2 \left(\Lambda_{,mnac} K^{(1)}_{(mi)(nj),(ab)(cd)} + \Lambda_{ac,mn} L^{(1)}_{(mi)(nj),(ab)(cd)} \right)$$
$$+ z_0 \Lambda_{ac}\delta_{mn}\delta_{ij} \left(K^{(0)}_{,(ab)(cd)} + L^{(0)}_{,(ab)(cd)} \right),$$
$$\Pi^{r}_{(mi),(Ab)(cd)} = r_0 \left(\Lambda_{A,mc} K^{(0)}_{(mi),(Ab)(cd)} - \Lambda_{C,Am} L^{(0)}_{(mi),(Ab)(cd)} \right),$$
$$\Pi^{pr}_{(Mi),(nj),(Ab)(cd)} = r_0^2 \left(\Lambda_{AM,nc} K^{(1)}_{(Mi)(nj),(Ab)(cd)} - \Lambda_{Mc,An} L^{(1)}_{(Mi)(nj),(Ab)(cd)} \right),$$

where

$$L^{(m)}_{(ij)\ldots(kl),(ab)(cd)} = \int_0^1 r f_{ij} \ldots f_{kl}\, G^{(m)}_{(ab)(cd)}\, \mathrm{d}r; \quad K^{(m)}_{(ij)\ldots(kl),(ab)(cd)} = \int_0^1 r f_{ij} \ldots f_{kl}\, H^{(m)}_{(ab)(cd)}\, \mathrm{d}r$$

with

$$G^{(0)}_{(ab)(cd)}(r) = \frac{ab}{r^2} f_{ab} f_{cd}; \quad H^{(0)}_{(ab)(cd)}(r) = r_0^2 \left[f^r_{ab} f^r_{cd} + \kappa_{ab}\kappa_{cd} f_{ab} f_{cd} \right],$$
$$G^{(1)}_{(ab)(cd)}(r) = \frac{ab}{r^2} \left[f_{ab} \left(\kappa_{cd} f_{cd} - r \frac{z_0}{r_0} f^r_{cd} \right) + f_{cd} \left(\kappa_{ab} f_{ab} - r \frac{z_0}{r_0} f^r_{ab} \right) \right]$$

https://doi.org/10.1017/jfm.2012.635 Published online by Cambridge University Press

$$H^{(1)}_{(ab)(cd)}(r) = -2z_0\left[f^r_{ab}f^r_{cd} + \kappa_{ab}\kappa_{cd}f_{ab}f_{cd}\right] + r_0^2\left[f^r_{cd}\left(\kappa_{ab}f^r_{ab} - r\frac{z_0}{r_0}f^{rr}_{ab}\right)\right.$$
$$+ f^r_{ab}\left(\kappa_{cd}f^r_{cd} - r\frac{z_0}{r_0}f^{rr}_{cd}\right) + \kappa_{cd}f_{cd}\left(\frac{a^2}{r^2r_0^2}f_{ab} - f^{rr}_{ab} - \frac{1+z_0\kappa_{ab}r^2}{rr_0}f^r_{ab}\right)$$
$$\left. + \kappa_{ab}f_{ab}\left(\frac{c^2}{r^2r_0^2}f_{cd} - f^{rr}_{cd} - \frac{1+z_0\kappa_{cd}r^2}{rr_0}f^r_{cd}\right)\right].$$

Even though we will account for the singular character of the second derivative and division by r^2, all of the required integrals are finite.

A.3. *Resolving the kinematic modal equations with respect to P_{Mi} and R_{mi}*

After substituting (3.18) into the kinematic equations and accounting for (A 5) and (A 6), gathering the same quantities gives

$$V^{pp}_{(Mi),(Nj),(Ab)} = \frac{1}{r_0^2\Lambda_{AA}\kappa_{Ab}}\left[\chi^{pp}_{(Nj)(Mi),(Ab)} - \frac{r_0\Pi^{p,p}_{(Nj),(Ab)(Mi)}}{\kappa_{Mi}}\right],$$

$$V^{rr}_{(mi),(nj),(Ab)} = \frac{1}{r_0^2\Lambda_{AA}\kappa_{Ab}}\left[\chi^{rr}_{(nj)(mi),(Ab)} - \frac{r_0\Pi^{r}_{(nj),(Ab)(mi)}}{\kappa_{mi}}\right],$$

$$V^{rp}_{(nj),(Mi),(ab)} = \frac{1}{r_0^2\Lambda_{aa}\kappa_{ab}}\left[\chi^{pr}_{(Mi),(nj),(ab)} - \frac{r_0\Pi^{r,p}_{(Mi),(ab)(nj)}}{\kappa_{nj}}\right],$$

$$V^{pr}_{(Mi),(nj),(ab)} = \frac{1}{r_0^2\Lambda_{aa}\kappa_{ab}}\left[\chi^{pr}_{(Mi),(nj),(ab)} - \frac{r_0\Pi^{r}_{(nj),(Mi)(ab)}}{\kappa_{Mi}}\right],$$

$$V^{ppp}_{(Mi),(Nj),(Kl),(Ab)} = \frac{1}{r_0^2\Lambda_{AA}\kappa_{Ab}}\left[\chi^{ppp}_{(Mi)(Nj)(Kl),(Ab)} - \frac{r_0\Pi^{p,pp}_{(Nj)(Kl),(Ab)(Mi)}}{\kappa_{Mi}}\right.$$
$$\left. - \sum_{Cd} V^{pp}_{(Mi),(Nj),(Cd)}\Pi^{p,p}_{(Kl),(Ab)(Cd)}\right];$$

$$V^{prr}_{(Mi),(nj),(kl),(Ab)} = \frac{1}{r_0^2\Lambda_{AA}\kappa_{Ab}}\left[\chi^{prr}_{(Mi),(nj)(kl),(Ab)} - \frac{r_0\Pi^{p,rr}_{(nj)(kl),(Ab)(Mi)}}{\kappa_{Mi}}\right.$$
$$\left. - \sum_{cd} V^{pr}_{(Mi),(nj),(cd)}\Pi^{r}_{(kl),(Ab)(cd)}\right],$$

$$V^{rrr}_{(mi),(nj),(kl),(ab)} = \frac{1}{r_0^2\Lambda_{aa}\kappa_{ab}}\left[\chi^{rrr}_{(nj)(kl)(mi),(ab)} - \frac{r_0\Pi^{r,rr}_{(nj)(kl),(ab)(mi)}}{\kappa_{mi}}\right.$$
$$\left. - \sum_{Cd} V^{rr}_{(mi),(nj),(Cd)}\Pi^{r}_{(kl),(Cd)(ab)}\right];$$

$$V^{rpp}_{(kl),(Mi),(Nj),(ab)} = \frac{1}{r_0^2\Lambda_{aa}\kappa_{ab}}\left[\chi^{ppr}_{(Mi)(Nj),(kl),(ab)} - \frac{r_0\Pi^{r,pp}_{(Mi)(Nj),(ab)(kl)}}{\kappa_{kl}}\right.$$
$$\left. - \sum_{cd} V^{rp}_{(kl),(Mi),(cd)}\Pi^{r,p}_{(Nj),(ab)(cd)}\right],$$

https://doi.org/10.1017/jfm.2012.635 Published online by Cambridge University Press

$$V^{ppr}_{(Mi),(Nj),(kl),(ab)} = \frac{1}{r_0^2 \Lambda_{aa}\kappa_{ab}}\left[2\chi^{ppr}_{(Mi)(Nj),(kl),(ab)} - \frac{r_0 \Pi^{pr}_{(Nj),(kl),(Mi)(ab)}}{\kappa_{Mi}} - \sum_{Cd} V^{pp}_{(Mi),(Nj),(Cd)}\Pi^{r}_{(kl),(Cd)(ab)} - \sum_{cd} V^{pr}_{(Mi),(kl),(cd)}\Pi^{r,p}_{(Nj),(ab)(cd)}\right],$$

$$V^{rpr}_{(nj),(Mi),(kl),(Ab)} = \frac{1}{r_0^2 \Lambda_{AA}\kappa_{Ab}}\left[2\chi^{prr}_{(Mi),(kl)(nj),(Ab)} - \frac{r_0 \Pi^{pr}_{(Mi),(kl),(Ab)(nj)}}{\kappa_{nj}} - \sum_{Cd} V^{rr}_{(nj),(kl),(Cd)}\Pi^{p,p}_{(Mi),(Ab)(Cd)} - \sum_{cd} V^{rp}_{(nj),(Mi),(cd)}\Pi^{r}_{(kl),(Ab)(cd)}\right].$$

A.4. *Dynamic modal equations with respect to p_{Mi} and r_{mi}*

We expand

$$\begin{aligned}\frac{\partial l_3}{\partial p_{Cd}} &= r_0^4 \Lambda_{CC} p_{Cd} + \sum_{MN,ij} T^{pp}_{(Mi)(Nj),(Cd)} p_{Mi} p_{Nj} + \sum_{mnij} T^{rr}_{(mi)(nj),(Cd)} r_{mi} r_{nj} \\ &\quad + \sum_{MNK,ijl} T^{ppp}_{(Mi)(Nj)(Kl),(Cd)} p_{Mi} p_{Nj} p_{Kl} + \sum_{M,nkijl} T^{prr}_{(Mi)(nj)(kl),(Cd)} p_{Mi} r_{nj} r_{kl}, \\ \frac{\partial l_3}{\partial r_{cd}} &= r_0^4 \Lambda_{cc} p_{cd} + \sum_{M,nij} T^{pr}_{(Mi)(nj),(cd)} p_{Mi} r_{nj} + \sum_{mnkijl} T^{rrr}_{(mi)(nj)(kl),(cd)} r_{mi} r_{nj} r_{kl} \\ &\quad + \sum_{MN,kijl} T^{prr}_{(Mi)(Nj)(kl),(cd)} p_{Mi} p_{Nj} r_{kl},\end{aligned} \tag{A 7}$$

where

$$\begin{aligned} T^{ppp}_{(Mi)(Nj)(Kl),(Cd)} &= -r_0^4 \Lambda_{MNKC,}\, \lambda_{(Mi)(Nj)(Kl)(Cd)} - \frac{2z_0^2 r_0^2}{\pi}\left[\Lambda_{CM}\delta_{id}\Lambda_{NK}\delta_{jl} + \Lambda_{NC}\delta_{jd}\Lambda_{MK}\delta_{il} + \Lambda_{KC}\delta_{ld}\Lambda_{MN}\delta_{ij}\right]; \\ T^{pp}_{(Mi)(Nj),(Cd)} &= -2z_0 r_0^3 \Lambda_{MNC,}\, \lambda_{(Mi)(Nj)(Cd)}, \\ T^{prr}_{(Mi),(nj)(kl),(Cd)} &= -3r_0^4 \Lambda_{CM,nk}\lambda_{(Mi)(nj)(kl)(Cd)} - 6z_0^2 r_0^2 \Lambda_{CM}\delta_{id}\delta_{nk}\delta_{jl}, \\ T^{pr}_{(Mi),(nj),(cd)} &= -4z_0 r_0^3 \Lambda_{M,nc}\lambda_{(Mi)(nj)(cd)}, \\ T^{rrr}_{(mi)(nj)(kl),(cd)} &= -r_0^4 \Lambda_{,mnkc}\lambda_{(mi)(nj)(kl)(cd)} - 2z_0^2 r_0^2 \pi[\delta_{cm}\delta_{id}\delta_{nk}\delta_{jl} + \delta_{nc}\delta_{jd}\delta_{mk}\delta_{il} + \delta_{kl}\delta_{ld}\delta_{mn}\delta_{ij}]; \\ T^{rr}_{(mi)(nj),(Cd)} &= -2z_0 r_0^3 \Lambda_{C,mn}\, \lambda_{(mi)(nj)(Cd)}, \\ T^{ppr}_{(Mi)(Nj),(kl)(cd)} &= -3r_0^4 \Lambda_{MN,kc}\lambda_{(Mi)(Nj)(kl)(cd)} - 6z_0^2 r_0^2 \Lambda_{MN}\delta_{ij}\delta_{kc}\delta_{ld}, \end{aligned}$$

and remark that $\partial l_1/\partial \bullet_{**}$ and $\partial l_2/\partial \bullet_{**}$ at the forcing terms require only the $O(1)$ components within the framework of the third-order approximation whose non-zeros are

$$\frac{\partial l_1}{\partial p_{1b}} = \frac{\partial l_2}{\partial r_{1b}} = \pi r_0^4 e_b, \quad e_b = \int_0^1 r^2 f_{1b}\,\mathrm{d}r. \tag{A 8}$$

To derive the final modal equations, we differentiate (3.18) and introduce

$$\begin{aligned} \bar{V}^{ppp}_{(Mi),(Nj),(Kl),(Ab)} &= V^{ppp}_{(Mi),(Nj),(Kl),(Ab)} + V^{ppp}_{(Mi),(Kl),(Nj),(Ab)}, \\ \bar{V}^{prr}_{(Mi),(nj),(kl),(Ab)} &= V^{prr}_{(Mi),(nj),(kl),(Ab)} + V^{prr}_{(Mi),(kl),(nj),(Ab)} + V^{rpr}_{(nj),(Mi),(kl),(Ab)}, \end{aligned}$$

https://doi.org/10.1017/jfm.2012.635 Published online by Cambridge University Press

$$\bar{V}^{pr}_{(Mi),(nj),(ab)} = V^{pr}_{(Mi),(nj),(ab)} + V^{rp}_{(nj),(Mi),(ab)},$$
$$\bar{V}^{rrr}_{(mi),(nj),(kl),(ab)} = V^{rrr}_{(mi),(nj),(kl),(ab)} + V^{rrr}_{(mi),(kl),(nj),(ab)},$$
$$\bar{V}^{rpp}_{(kl),(Mi),(Nj),(ab)} = V^{rpp}_{(kl),(Mi),(Nj),(ab)} + V^{rpp}_{(kl),(Nj),(Mi),(ab)} + V^{ppr}_{(Mi),(Nj),(kl),(ab)}.$$

Further, the cubic approximation

$$\frac{\partial A^{pp}_{(Ab)(Cd)}}{\partial p_{Ef}} = \Pi^{p,p}_{(Ef),(Ab)(Cd)} + 2\sum_{Mi} \Pi^{p,pp}_{(Mi)(Ef),(Ab)(Cd)} p_{Mi},$$
$$\frac{\partial A^{pp}_{(Ab)(Cd)}}{\partial r_{ef}} = 2\sum_{mi} \Pi^{p,rr}_{(mi)(ef),(Ab)(Cd)} r_{mi},$$
$$\frac{\partial A^{rr}_{(ab)(cd)}}{\partial p_{Ef}} = \Pi^{r,p}_{(Ef),(ab)(cd)} + 2\sum_{Mi} \Pi^{r,pp}_{(Mi)(Ef),(ab)(cd)} p_{Mi},$$
$$\frac{\partial A^{rr}_{(ab)(cd)}}{\partial r_{ef}} = 2\sum_{mi} \Pi^{r,rr}_{(mi)(ef),(ab)(cd)} r_{mi}; \qquad \frac{\partial A^{pr}_{(Ab),(cd)}}{\partial p_{Ef}} = \sum_{nj} \Pi^{pr}_{(Ef),(nj),(Ab)(cd)} r_{nj},$$
$$\frac{\partial A^{pr}_{(Ab),(cd)}}{\partial r_{ef}} = \Pi^{r}_{(ef),(Ab)(cd)} + \sum_{Mi} \Pi^{pr}_{(Mi),(ef),(Ab)(cd)} p_{Mi}$$

should be substituted in (3.11) where we should keep the only cubic polynomials in the generalized coordinates. This leads to weakly nonlinear modal equations (3.19) whose coefficients are

$$d^{pp,(Ef)}_{(Mi),(Nj)} = \frac{\kappa_{Ef}}{r_0^3 \Lambda_{EE}} \left[r_0^2 \Lambda_{EE} V^{pp}_{(Mi),(Nj),(Ef)} + \frac{\chi^{pp}_{(Nj)(Ef),(Mi)}}{\kappa_{Mi}} \right],$$
$$d^{ppp,(Ef)}_{(Mi),(Nj),(Kl)} = \frac{\kappa_{Ef}}{r_0^4 \Lambda_{EE}} \left[r_0^3 \Lambda_{EE} V^{ppp}_{(Mi),(Nj),(Kl),(Ef)} + \frac{r_0 \chi^{ppp}_{(Ef)(Nj)(Kl),(Mi)}}{\kappa_{Mi}} + \sum_{Ab} V^{pp}_{(Mi),(Nj),(Ab)} \chi^{pp}_{(Kl)(Ef),(Ab)} \right],$$
$$d^{prr,(Ef)}_{(Mi),(nj),(kl)} = \frac{\kappa_{Ef}}{r_0^4 \Lambda_{EE}} \left[r_0^3 \Lambda_{EE} V^{prr}_{(Mi),(nj),(kl),(Ef)} + \frac{r_0 \chi^{prr}_{(Ef),(nj)(kl),(Mi)}}{\kappa_{Mi}} + \sum_{ab} V^{pr}_{(Mi),(nj),(ab)} \chi^{pr}_{(Ef),(kl),(ab)} \right],$$
$$d^{rr,(Ef)}_{(mi),(nj)} = \frac{\kappa_{Ef}}{r_0^3 \Lambda_{EE}} \left[r_0^2 \Lambda_{EE} V^{rr}_{(mi),(nj),(Ef)} + \frac{\chi^{pr}_{(Ef),(nj),(mi)}}{\kappa_{mi}} \right],$$
$$d^{rrp,(Ef)}_{(mi),(nj),(Kl)} = \frac{\kappa_{Ef}}{r_0^4 \Lambda_{EE}} \left[r_0^3 \Lambda_{EE} V^{rpr}_{(mi),(Kl),(nj),(Ef)} + \frac{2 r_0 \chi^{ppr}_{(Kl)(Ef),(nj),(mi)}}{\kappa_{mi}} + \sum_{ab} V^{rp}_{(mi),(Kl),(ab)} \chi^{pr}_{(Ef),(nj),(ab)} + \sum_{Ab} V^{rr}_{(mi),(nj),(Ab)} \chi^{pp}_{(Kl)(Ef),(Ab)} \right],$$
$$t^{pp,(Ef)}_{(Mi),(Nj)} = \frac{\kappa_{Ef}}{r_0^2 \Lambda_{EE}} \left[r_0 \Lambda_{EE} V^{pp}_{(Mi),(Nj),(Ef)} + \frac{\Pi^{p,p}_{(Ef),(Mi)(Nj)}}{2\kappa_{Mi}\kappa_{Nj}} \right],$$

https://doi.org/10.1017/jfm.2012.635 Published online by Cambridge University Press

$$t^{ppp,(Ef)}_{(Mi),(Nj),(Kl)} = \frac{\kappa_{Ef}}{r_0^4 \Lambda_{EE}} \left[r_0^3 \Lambda_{EE} \bar{V}^{ppp}_{(Mi),(Nj),(Kl),(Ef)} + \frac{r_0^2 \Pi^{p,pp}_{(Kl)(Ef),(Mi)(Nj)}}{\kappa_{Mi}\kappa_{Nj}} + \sum_{Ab} V^{pp}_{(Mi),(Nj),(Ab)} \chi^{pp}_{(Kl)(Ef),(Ab)} + \sum_{Ab} \frac{r_0 \Pi^{p,p}_{(Ef),(Mi)(Ab)}}{\kappa_{Mi}} V^{pp}_{(Nj),(Kl),(Ab)} \right],$$

$$t^{rr,(Ef)}_{(mi),(nj)} = \frac{\kappa_{Ef}}{r_0^2 \Lambda_{EE}} \left[r_0 \Lambda_{EE} V^{rr}_{(mi),(nj),(Ef)} + \frac{\Pi^{r,p}_{(Ef),(mi)(nj)}}{2\kappa_{mi}\kappa_{nj}} \right],$$

$$t^{rrp,(Ef)}_{(mi),(nj),(Kl)} = \frac{\kappa_{Ef}}{r_0^4 \Lambda_{EE}} \left[r_0^3 \Lambda_{EE} V^{rpr}_{(mi),(Kl),(nj),(Ef)} + \frac{r_0^2 \Pi^{r,pp}_{(Kl)(Ef),(mi)(nj)}}{\kappa_{mi}\kappa_{nj}} + \sum_{Ab} V^{rr}_{(mi),(nj),(Ab)} \chi^{pp}_{(Kl)(Ef),(Ab)} + \sum_{ab} \frac{r_0 \Pi^{r,p}_{(Ef),(mi)(ab)}}{\kappa_{mi}} V^{rp}_{(nj),(Kl),(ab)} \right],$$

$$t^{prr,(Ef)}_{(Mi),(nj),(kl)} = \frac{\kappa_{Ef}}{r_0^4 \Lambda_{EE}} \left[r_0^3 \Lambda_{EE} \bar{V}^{prr}_{(Mi),(nj),(kl),(Ef)} + \frac{r_0^2 \Pi^{pr}_{(Ef),(kl),(Mi)(nj)}}{\kappa_{Mi}\kappa_{nj}} + \sum_{ab} \left(\bar{V}^{pr}_{(Mi),(nj),(ab)} \chi^{pr}_{(Ef),(kl),(ab)} + \frac{r_0}{\kappa_{nj}} V^{pr}_{(Mi),(kl),(ab)} \Pi^{r,p}_{(Ef),(ab)(nj)} \right) + \sum_{Ab} \frac{r_0 \Pi^{p,p}_{(Ef),(Mi)(Ab)}}{\kappa_{Mi}} V^{rr}_{(nj),(kl),(Ab)} \right],$$

$$g^{pp,(Ef)}_{(Mi)(Nj)} = -\frac{2z_0\kappa_{Ef}}{r_0 \Lambda_{EE}} \Lambda_{MNE,} \lambda_{(Mi)(Nj)(Ef)}; \quad g^{rr,(Ef)}_{(mi)(nj)} = -\frac{2z_0\kappa_{Ef}}{r_0 \Lambda_{EE}} \Lambda_{E,mn} \lambda_{(mi)(nj)(Ef)},$$

$$g^{ppp,(Ef)}_{(Mi)(Nj)(Kl)} = \frac{\kappa_{Ef}}{r_0^2 \Lambda_{EE}} \left[-r_0^2 \Lambda_{MNKE,} \lambda_{(Mi)(Nj)(Kl)(Ef)} - 2z_0^2 \pi^{-1} (\Lambda_{EM}\delta_{if}\Lambda_{NK}\delta_{jl} + \Lambda_{NE}\delta_{jf}\Lambda_{MK}\delta_{il} + \Lambda_{KE}\delta_{lf}\Lambda_{MN}\delta_{ij}) \right],$$

$$g^{prr,(Ef)}_{(Mi),(nj),(kl)} = -\frac{3\kappa_{Ef}}{r_0^2 \Lambda_{EE}} \left[r_0^2 \Lambda_{EM,nk} \lambda_{(Mi)(nj)(kl)(Ef)} + 2z_0^2 \Lambda_{EM} \delta_{if}\delta_{nk}\delta_{jl} \right];$$

$$d^{pr,(ef)}_{(Mi),(nj)} = \frac{\kappa_{ef}}{r_0^3 \Lambda_{ee}} \left[r_0^2 \Lambda_{ee} V^{pr}_{(Mi),(nj),(ef)} + \frac{\chi^{rr}_{(nj),(ef),(Mi)}}{\kappa_{Mi}} \right],$$

$$d^{prp,(ef)}_{(Mi),(nj),(Kl)} = \frac{\kappa_{ef}}{r_0^4 \Lambda_{ee}} \left[r_0^3 \Lambda_{ee} V^{ppr}_{(Mi),(Kl),(nj),(ef)} + \frac{2r_0 \chi^{prr}_{(Kl),(nj)(ef),(Mi)}}{\kappa_{Mi}} + \sum_{Ab} V^{pp}_{(Mi),(Kl),(Ab)} \chi^{rr}_{(nj)(ef),(Ab)} + \sum_{ab} V^{pr}_{(Mi),(nj),(ab)} \chi^{pr}_{(Kl),(ef),(ab)} \right],$$

$$d^{rp,(ef)}_{(mi),(Nj)} = \frac{\kappa_{ef}}{r_0^3 \Lambda_{ee}} \left[r_0^2 \Lambda_{ee} V^{rp}_{(mi),(Nj),(ef)} + \frac{\chi^{pr}_{(Nj),(ef),(mi)}}{\kappa_{mi}} \right],$$

$$d^{rpp,(ef)}_{(mi),(Nj),(Kl)} = \frac{\kappa_{ef}}{r_0^4 \Lambda_{ee}} \left[r_0^3 \Lambda_{ee} V^{rpp}_{(mi),(Nj),(Kl),(ef)} + \frac{r_0 \chi^{ppr}_{(Nj)(Kl),(ef),(mi)}}{\kappa_{mi}} + \sum_{ab} V^{rp}_{(mi),(Nj),(ab)} \chi^{pr}_{(Kl),(ef),(ab)} \right],$$

https://doi.org/10.1017/jfm.2012.635 Published online by Cambridge University Press

$$d^{rrr,(ef)}_{(mi),(nj),(kl)} = \frac{\kappa_{ef}}{r_0^4\Lambda_{ee}}\left[r_0^3\Lambda_{ee}V^{rrr}_{(mi),(nj),(kl),(ef)} + \frac{r_0\chi^{rrr}_{(nj)(kl)(ef),(mi)}}{\kappa_{mi}} + \sum_{Ab} V^{rr}_{(mi),(nj),(Ab)}\chi^{rr}_{(kl)(ef),(Ab)}\right],$$

$$t^{pr,(ef)}_{(Mi),(nj)} = \frac{\kappa_{ef}}{r_0^2\Lambda_{ee}}\left[r_0\Lambda_{ee}\bar{V}^{pr}_{(Mi),(nj),(ef)} + \frac{\Pi^{r}_{(ef),(Mi)(nj)}}{\kappa_{Mi}\kappa_{nj}}\right],$$

$$t^{prp,(ef)}_{(Mi),(nj),(Kl)} = \frac{\kappa_{ef}}{r_0^4\Lambda_{ee}}\left[r_0^3\Lambda_{ee}\bar{V}^{rpp}_{(nj),(Mi),(Kl),(ef)} + \frac{r_0^2\Pi^{pr}_{(Kl),(ef),(Mi)(nj)}}{\kappa_{Mi}\kappa_{nj}} + \sum_{ab}\bar{V}^{pr}_{(Mi),(nj),(ab)}\chi^{pr}_{(Kl),(ef),(ab)} + \sum_{ab}\frac{r_0V^{rp}_{(nj),(Kl),(ab)}}{\kappa_{Mi}}\Pi^{r}_{(ef),(Mi)(ab)} + \sum_{Ab}\frac{r_0V^{pp}_{(Mi),(Kl),(Ab)}}{\kappa_{nj}}\Pi^{r}_{(ef),(Ab)(nj)}\right],$$

$$t^{ppr,(ef)}_{(Mi),(Nj),(kl)} = \frac{\kappa_{ef}}{r_0^4\Lambda_{ee}}\left[r_0^3\Lambda_{ee}V^{ppr}_{(Mi),(Nj),(kl),(ef)} + \frac{r_0^2\Pi^{p,rr}_{(kl)(ef),(Mi)(Nj)}}{\kappa_{Mi}\kappa_{Nj}} + \sum_{Ab}V^{pp}_{(Mi),(Nj),(Ab)}\chi^{rr}_{(kl)(ef),(Ab)} + \sum_{ab}\frac{r_0V^{pr}_{(Nj),(kl),(ab)}}{\kappa_{Mi}}\Pi^{r}_{(ef),(Mi)(ab)}\right],$$

$$t^{rrr,(ef)}_{(mi),(nj),(kl)} = \frac{\kappa_{ef}}{r_0^4\Lambda_{ee}}\left[r_0^3\Lambda_{ee}\bar{V}^{rrr}_{(mi),(nj),(kl),(ef)} + \frac{r_0^2\Pi^{r,rr}_{(kl)(ef),(mi)(nj)}}{\kappa_{mi}\kappa_{nj}} + \sum_{Ab}V^{rr}_{(mi),(nj),(Ab)}\chi^{rr}_{(kl)(ef),(Ab)} + \sum_{Ab}\frac{r_0V^{rr}_{(mi),(kl),(Ab)}}{\kappa_{nj}}\Pi^{r}_{(ef),(Ab)(nj)}\right],$$

$$g^{rp(ef)}_{(mi),(Nj)} = -\frac{4z_0\kappa_{ef}}{r_0\Lambda_{ee}}\Lambda_{N,me}\lambda_{(Nj)(mi)(ef)},$$

$$g^{rpp,(ef)}_{(mi),(Nj)(Kl)} = -\frac{3\kappa_{ef}}{r_0^2\Lambda_{ee}}\left[r_0^2\Lambda_{NK,me}\lambda_{(Nj)(Kl)(mi)(ef)} + 2z_0^2\Lambda_{KN}\delta_{jl}\delta_{me}\delta_{if}\right],$$

$$g^{rrr,(ef)}_{(mi)(nj)(kl)} = -\frac{\kappa_{ef}}{r_0^2\Lambda_{ee}}[r_0^2\Lambda_{,mnke}\lambda_{(mi)(nj)(kl)(ef)} + 2z_0^2\pi(\delta_{em}\delta_{if}\delta_{nk}\delta_{jl} + \delta_{ne}\delta_{jf}\delta_{mk}\delta_{il} + \delta_{ke}\delta_{lf}\delta_{mn}\delta_{ij})].$$

Appendix B. Non-zero coefficients in the Moiseev–Narimanov modal equations

For the d-type coefficients,

$$d_1 = d^{ppp,(11)}_{(11),(11),(11)} = d^{rrr,(11)}_{(11),(11),(11)} = t^{ppp,(11)}_{(11),(11),(11)} = t^{rrr,(11)}_{(11),(11),(11)},$$

$$d_2 = d^{prr,(11)}_{(11),(11),(11)} = d^{rpp,(11)}_{(11),(11),(11)} = \tfrac{1}{2}t^{prr,(11)}_{(11),(11),(11)} = \tfrac{1}{2}t^{prp,(11)}_{(11),(11),(11)},$$

$$d_1 - d_2 = d^{rrp,(11)}_{(11),(11),(11)} = d^{prp,(11)}_{(11),(11),(11)}; \quad d_1 - 2d_2 = t^{rrp,(11)}_{(11),(11),(11)} = t^{ppr,(11)}_{(11),(11),(11)},$$

$$d_3^{(j)} = d^{pp,(11)}_{(11),(2j)} = d^{rr,(11)}_{(11),(2j)} = d^{pr,(11)}_{(11),(2j)} = -d^{rp,(11)}_{(11),(2j)} = t^{pr,(11)}_{(11),(2j)} = -t^{pr,(11)}_{(2j),(11)} = t^{pp,(11)}_{(11),(2j)} + t^{pp,(11)}_{(2j),(11)} = t^{rr,(11)}_{(11),(2j)} + t^{rr,(11)}_{(2j),(11)},$$

https://doi.org/10.1017/jfm.2012.635 Published online by Cambridge University Press

$$d_4^{(j)} = d^{pp,(11)}_{(2j),(11)} = d^{rr,(11)}_{(2j),(11)} = -d^{pr,(11)}_{(2j),(11)} = d^{rp,(11)}_{(2j),(11)},$$

$$d_5^{(j)} = d^{pp,(11)}_{(11),(0j)} = d^{rp,(11)}_{(11),(0j)} = t^{pr,(11)}_{(0j),(11)} = t^{pp,(11)}_{(0j),(11)} + t^{pp,(11)}_{(11),(0j)};$$

$$d_6^{(j)} = d^{pp,(11)}_{(0j),(11)} = d^{pr,(11)}_{(0j),(11)},$$

$$d_{7,k} = t^{pp,(2k)}_{(11),(11)} = -t^{rr,(2k)}_{(11),(11)} = \tfrac{1}{2} t^{pr,(2k)}_{(11),(11)}; \quad d_{8,k} = t^{pp,(0k)}_{(11),(11)} = t^{rr,(0k)}_{(11),(11)},$$

$$d_{9,k} = d^{pp,(2k)}_{(11),(11)} = -d^{rr,(2k)}_{(11),(11)} = d^{pr,(2k)}_{(11),(11)} = d^{rp,(2k)}_{(11),(11)};$$

$$d_{10,k} = d^{pp,(0k)}_{(11),(11)} = d^{rr,(0k)}_{(11),(11)},$$

$$d_{11,k} = d^{ppp,(3k)}_{(11),(11),(11)} = -d^{rrr,(3k)}_{(11),(11),(11)} = -\tfrac{1}{2} d^{rrp,(3k)}_{(11),(11),(11)},$$

$$d_{12,k} = t^{ppp,(3k)}_{(11),(11),(11)} = -t^{rrp,(3k)}_{(11),(11),(11)} = -\tfrac{1}{2} t^{prr,(3k)}_{(11),(11),(11)} = t^{ppr,(3k)}_{(11),(11),(11)}$$
$$= -t^{rrr,(3k)}_{(11),(11),(11)} = \tfrac{1}{2} t^{prp,(3k)}_{(11),(11),(11)};$$

$$d_{13,k}^{(j)} = d^{pp,(3k)}_{(11),(2j)} = -d^{rr,(3k)}_{(11),(2j)} = d^{pr,(3k)}_{(11),(2j)} = d^{rp,(3k)}_{(11),(2j)},$$

$$d_{14,k}^{(j)} = d^{pp,(3k)}_{(2j),(11)} = -d^{rr,(3k)}_{(2j),(11)} = d^{pr,(3k)}_{(2j),(11)} = d^{rp,(3k)}_{(2j),(11)},$$

$$d_{15,k}^{(j)} = t^{pp,(3k)}_{(11),(2j)} + t^{pp,(3k)}_{(2j),(11)} = -t^{rr,(3k)}_{(11),(2j)} - t^{rr,(3k)}_{(2j),(11)} = t^{pr,(3k)}_{(11),(2j)} = t^{pr,(3k)}_{(2j),(11)},$$

$$d_{16,n} = d^{ppp,(1n)}_{(11),(11),(11)} = d^{rrr,(1n)}_{(11),(11),(11)}, \quad d_{17,n} = d^{prr,(1n)}_{(11),(11),(11)} = d^{rpp,(1n)}_{(11),(11),(11)},$$

$$d_{16,n} - d_{17,n} = d^{rrp,(1n)}_{(11),(11),(11)} = d^{prp,(1n)}_{(11),(11),(11)}; \quad d_{18,n} = t^{ppp,(1n)}_{(11),(11),(11)} = t^{rrr,(1n)}_{(11),(11),(11)},$$

$$d_{19,n} = t^{prr,(1n)}_{(11),(11),(11)} = t^{prp,(1n)}_{(11),(11),(11)}; \quad d_{18,n} - d_{19,n} = t^{rrp,(1n)}_{(11),(11),(11)} = t^{ppr,(1n)}_{(11),(11),(11)},$$

$$d_{20,n}^{(j)} = d^{pp,(1n)}_{(11),(2j)} = d^{rr,(1n)}_{(11),(2j)} = d^{pr,(1n)}_{(11),(2j)} = -d^{rp,(1n)}_{(11),(2j)},$$

$$d_{21,n}^{(j)} = d^{pp,(1n)}_{(2j),(11)} = d^{rr,(1n)}_{(2j),(11)} = -d^{pr,(1n)}_{(2j),(11)} = d^{rp,(1n)}_{(2j),(11)},$$

$$d_{22,n}^{(j)} = t^{pp,(1n)}_{(11),(2j)} + t^{pp,(1n)}_{(2j),(11)} = t^{rr,(1n)}_{(11),(2j)} + t^{rr,(1n)}_{(2j),(11)} = t^{pr,(1n)}_{(11),(2j)} = -t^{pr,(1n)}_{(2j),(11)},$$

$$d_{23,n}^{(j)} = d^{pp,(1n)}_{(11),(0j)} = d^{rp,(1n)}_{(11),(0j)}; \quad d_{24,n}^{(j)} = d^{pp,(1n)}_{(0j),(11)} = d^{pr,(1n)}_{(0j),(11)},$$

$$d_{25,n}^{(j)} = t^{pp,(1n)}_{(11),(0j)} + t^{pp,(1n)}_{(0j),(11)} = t^{pr,(1n)}_{(0j),(11)}$$

and the $\mathscr{G}$ coefficients are computed by

$$\sigma_{11}^2 \mathscr{G}_1 = g^{ppp,(11)}_{(11),(11),(11)} = g^{rrr,(11)}_{(11),(11),(11)} = g^{rpp,(11)}_{(11),(11),(11)} = g^{prr,(11)}_{(11),(11),(11)},$$

$$\sigma_{1n}^2 \mathscr{G}_{1,n} = g^{ppp,(1n)}_{(11),(11),(11)} = g^{rrr,(1n)}_{(11),(11),(11)} = g^{prr,(1n)}_{(11),(11),(11)} = g^{rpp,(1n)}_{(11),(11),(11)},$$

$$\sigma_{11}^2 \mathscr{G}_2^{(j)} = 2g^{pp,(11)}_{(11),(2j)} = 2g^{rr,(11)}_{(11),(2j)} = g^{rp,(11)}_{(2j),(11)} = -g^{rp,(11)}_{(11),(2j)},$$

$$\sigma_{1n}^2 \mathscr{G}_{2,n}^{(j)} = 2g^{pp,(1n)}_{(11),(2j)} = 2g^{rr,(1n)}_{(11),(2j)} = -g^{rp,(1n)}_{(11),(2j)} = g^{rp,(1n)}_{(2j),(11)},$$

$$\sigma_{11}^2 \mathscr{G}_3^{(j)} = 2g^{pp,(11)}_{(11),(0j)} = g^{rp,(11)}_{(11),(0j)}; \quad \sigma_{1n}^2 \mathscr{G}_{3,n}^{(j)} = 2g^{pp,(1n)}_{(11),(0j)} = g^{rp,(1n)}_{(11),(0j)},$$

$$\sigma_{2k}^2 \mathscr{G}_{4,k} = g^{pp,(2k)}_{(11),(11)} = -g^{rr,(2k)}_{(11),(11)} = \tfrac{1}{2} g^{rp,(2k)}_{(11),(11)}; \quad \sigma_{0k}^2 \mathscr{G}_{5,k} = g^{pp,(0k)}_{(11),(11)} = g^{rr,(0k)}_{(11),(11)},$$

$$\sigma_{3k}^2 \mathscr{G}_{6,k} = g^{ppp,(3k)}_{(11),(11),(11)} = -g^{rrr,(3k)}_{(11),(11),(11)} = \tfrac{1}{3} g^{rpp,(3k)}_{(11),(11),(11)} = -\tfrac{1}{3} g^{prr,(3k)}_{(11),(11),(11)},$$

$$\sigma_{3k}^2 \mathscr{G}_{7,k}^{(j)} = 2g^{pp,(3k)}_{(11),(2j)} = -2g^{rr,(3k)}_{(11),(2j)} = g^{rp,(3k)}_{(11),(2j)} = g^{rp,(3k)}_{(2j),(11)} \quad \text{where } k, j \geqslant 1 \text{ and } n \geqslant 2.$$

Here σ_{Mi} are the non-dimensional natural sloshing frequencies defined from the spectral boundary problem on the natural sloshing modes.

https://doi.org/10.1017/jfm.2012.635 Published online by Cambridge University Press

REFERENCES

ANSARI, M. R., FIROUZ-ABADI, R. D. & GHASEMI, M. 2011 Two phase modal analysis of nonlinear sloshing in a rectangular container. *Ocean Engng* **38** (11–12), 1277–1282.

ANTUONO, M., BOUSCASSE, B., COLAGROSSI, A. & LUGNI, C. 2012 Two-dimensional modal method for shallow-water sloshing in rectangular basins. *J. Fluid Mech.* **700**, 419–440.

BARNYAK, M., GAVRILYUK, I., HERMANN, M. & TIMOKHA, A. 2011 Analytical velocity potentials in cells with a rigid spherical wall. *Z. Angew. Math. Mech.* **91** (1), 38–45.

BATEMAN, H. 1944 *Partial Differential Equations of Mathematical Physics*. Dover.

BUDIANSKY, B. 1958 Sloshing of liquids in circular canals and spherical tanks. *Tech. Rep.* Lockheed Aircraft Corporation, Missile System Division, Sunnyvale, California.

BUDIANSKY, B. 1960 Sloshing of liquid in circular canals and spherical tanks. *J. Aerosp. Sci.* **27** (3), 161–172.

DRODOS, G. C., DIMAS, A. A. & KARABALIS, D. L. 2008 Discrete modes for seismic analysis of liquid storage tanks of arbitrary shape and height. *J. Pressure Vessel Technol.* **130**, 0418011.

EASTHAM, M. 1962 An eigenvalue problem with parameter in the boundary condition. *Q. J. Maths* **13**, 304–320.

FALTINSEN, O. M., FIROOZKOOHI, R. & TIMOKHA, A. N. 2011 Effect of central slotted screen with a high solidity ratio on the secondary resonance phenomenon for liquid sloshing in a rectangular tank. *Phys. Fluids* **23**, 062106.

FALTINSEN, O. M., ROGNEBAKKE, O. F. & TIMOKHA, A. N. 2003 Resonant three-dimensional nonlinear sloshing in a square base basin. *J. Fluid Mech.* **487**, 1–42.

FALTINSEN, O. M., ROGNEBAKKE, O. F. & TIMOKHA, A. N. 2005*a* Classification of three-dimensional nonlinear sloshing in a square-base tank with finite depth. *J. Fluids Struct.* **20** (1), 81–103.

FALTINSEN, O. M., ROGNEBAKKE, O. F. & TIMOKHA, A. N. 2005*b* Resonant three-dimensional nonlinear sloshing in a square base basin. Part 2. Effect of higher modes. *J. Fluid Mech.* **523**, 199–218.

FALTINSEN, O. M., ROGNEBAKKE, O. F. & TIMOKHA, A. N. 2006 Transient and steady-state amplitudes of resonant three-dimensional sloshing in a square base tank with a finite fluid depth. *Phys. Fluids* **18**, 012103.

FALTINSEN, O. M. & TIMOKHA, A. N. 2001 Adaptive multimodal approach to nonlinear sloshing in a rectangular tank. *J. Fluid Mech.* **432**, 167–200.

FALTINSEN, O. M. & TIMOKHA, A. N. 2009 *Sloshing*. Cambridge University Press.

FALTINSEN, O. M. & TIMOKHA, A. N. 2012 Analytically approximate natural sloshing modes for a spherical tank shape. *J. Fluid Mech.* **703**, 391–401.

GAVRILYUK, I., HERMANN, M., LUKOVSKY, I., SOLODUN, O. & TIMOKHA, A. 2008 Natural sloshing frequencies in rigid truncated conical tanks. *Engng Comput.* **25** (6), 518–540.

GAVRILYUK, I., LUKOVSKY, I. & TIMOKHA, A. N. 2000 A multimodal approach to nonlinear sloshing in a circular cylindrical tank. *Hybrid Methods Engng* **2** (4), 463–483.

GAVRILYUK, I., LUKOVSKY, I., TROTSENKO, YU. & TIMOKHA, A. 2007 Sloshing in a vertical circular cylindrical tank with an annular baffle. Part 2. Nonlinear resonant waves. *J. Engng Maths* **57**, 57–78.

GAVRILYUK, I. P., LUKOVSKY, I. A. & TIMOKHA, A. N. 2005 Linear and nonlinear sloshing in a circular conical tank. *Fluid Dyn. Res.* **37**, 399–429.

HARGNEAVES, R. 1908 A pressure-integral as kinetic potential. *Phil. Mag.* **16**, 436–444.

HASHEMINEJAD, S. M. & AGHABEIGI, M. 2009 Liquid sloshing in half-full horizontal elliptical tanks. *J. Sound Vib.* **324**, 332–349.

HYSING, T. 1976 Loads related to sloshing in spherical tanks. *Tech. Rep.* Det Norske Veritas, Hvik, Norway.

IKEDA, T. & IBRAHIM, R. A. 2005 Nonlinear random responses of a structure parametrically coupled with liquid sloshing in a cylindrical tank. *J. Sound Vib.* **284**, 75–102.

IKEDA, T., IBRAHIM, R. A., HARATA, Y. & KURIYAMA, T. 2012 Nonlinear liquid sloshing in a square tank subjected to obliquely horizontal excitation. *J. Fluid Mech.* **700**, 304–328.

https://doi.org/10.1017/jfm.2012.635 Published online by Cambridge University Press

KARAMANOS, S. A., PAPAPROKOPIOU, D. & PLATYRRACHOS, M. A. 2006 Sloshing effects on the seiesmic design of horizontal-cylindrical and spherical industrial vessels. *J. Pressure Vessel Technol.* **128**, 328–340.

KARAMANOS, S. A., PAPAPROKOPIOU, D. & PLATYRRACHOS, M. A. 2009 Finite element analysis of externally-induced sloshing in horizontal-cylindrical and axisymmetric liquid vessels. *J. Pressure Vessel Technol.* **131** (5)051301.

LA ROCCA, M., SCORTINO, M. & BONIFORTI, M. A. 2000 A fully nonlinear model for sloshing in a rotating container. *Fluid Dyn. Res.* **27**, 225–229.

LOVE, J. S. & TAIT, M. J. 2010 Nonlinear simulation of a tuned liquid damper with damping screens using a modal expansion technique. *J. Fluids Struct.* **26** (7–8), 1058–1077.

LOVE, J. S. & TAIT, M. J. 2011 Non-linear multimodal model for tuned liquid dampers of arbitrary tank geometry. *Intl J. Non-Linear Mech.* **46** (8), 1065–1075.

LUKE, J. C. 1967 A variational principle for a fluid with a free surface. *J. Fluid Mech.* **27**, 395–397.

LUKOVSKY, I. A. 1975 *Nonlinear Sloshing in Tanks of Complex Geometrical Shape*. Naukova Dumka (in Russian).

LUKOVSKY, I. A. 1990 *Introduction to Nonlinear Dynamics of Rigid Bodies with the Cavities Partially Filled by a Fluid*. Naukova Dumka (in Russian).

LUKOVSKY, I. A., OVCHYNNYKOV, D. V. & TIMOKHA, A. N. 2012 Asymptotic nonlinear multimodal method for liquid sloshing in an upright circular cylindrical tank. Part 1: modal equations. *Nonlinear Oscillations* **14** (4), 512–525.

LUKOVSKY, I. A. & TIMOKHA, A. N. 1995 Variational methods in nonlinear problems of the dynamics of a limited liquid volume. Institute of Mathematics of NASU, ISBN 5-7702-1184-9 (in Russian).

LUKOVSKY, I. A. & TIMOKHA, A. N. 2002 Modal modelling of nonlinear sloshing in tanks with non-vertical walls. Non-conformal mapping technique. *Intl J. Fluid Mech. Res.* **29** (2), 216–242.

LUKOVSKY, I. A., BARNYAK, M. Y. & KOMARENKO, A. N. 1984 *Approximate Methods of Solving the Problems of the Dynamics of a Limited Liquid Volume*. Naukova Dumka (in Russian).

MCIVER, P. 1989 Sloshing frequencies for cylindrical and spherical containers filled to an arbitrary depth. *J. Fluid Mech.* **201**, 243–257.

MILES, J. W. 1962 Stability of forced oscillations of a spherical pendulum. *Q. Appl. Maths* **20**, 21–32.

MILES, J. W. 1976 Nonlinear surface waves in closed basins. *J. Fluid Mech.* **75** (3), 419–448.

MILES, J. W. 1984*a* Internally resonant surface waves in circular cylinder. *J. Fluid Mech.* **149**, 1–14.

MILES, J. W. 1984*b* Resonantly forces surface waves in circular cylinder. *J. Fluid Mech.* **149**, 15–31.

MOISEEV, N. N. 1958 On the theory of nonlinear vibrations of a liquid of finite volume. *J. Appl. Math. Mech.* **22** (5), 860–872.

MOORE, R. E. & PERKO, L. M. 1964 Inviscid fluid flow in an accelerating cylindrical container. *J. Fluid Mech.* **22**, 305–320.

MORAND, J.-P. & OHAYON, R. 1995 *Fluid Structure Interaction. Applied Numerical Methods*. John Wiley & Sons.

NARIMANOV, G. S. 1957 Movement of a tank partly filled by a fluid: the taking into account of non-smallness of amplitude. *Prikl. Math. Mech.* **21**, 513–524.

PATKAS, L. & KARAMANOS, S. A. 2007 Variational solution of externally-induced sloshing in horizontal–cylindrical and spherical vessels. *J. Engng Mech.* **133** (6), 641–655.

PERKO, L. M. 1969 Large-amplitude motions of liquid–vapour interface in an accelerating container. *J. Fluid Mech.* **35**, 77–96.

STOFAN, A. J. & ARMSTED, A. L. 1962 Analytical and experimental investigation of forces and frequencies resulting from liquid sloshing in a spherical tank. *Tech. Rep.* D-1281. NASA, Lewis Research Center, Clevelend, Ohio.

SUMNER, I. E. 1966 Experimental investigations of stability boundaries for planar and nonplanar sloshing in spherical tanks. *Tech. Rep.* TN D-3210, NASA.

https://doi.org/10.1017/jfm.2012.635 Published online by Cambridge University Press

SUMNER, I. E. & STOFAN, A. J. 1963 An experimental investigation of the viscous damping of liquid sloshing in spherical tanks. *Tech. Rep.* TN D-1991, NASA Technical Note.

TAKAHARA, H., HARA, K. & ISHIDA, T. 2012 Nonlinear liquid oscillation in a cylindrical tank with an eccentric core barrel. *J. Fluids Struct.* **35**, 120–132.

TAKAHARA, H. & KIMURA, K. 2012 Frequency response of sloshing in an annular cylindrical tank subjected to pitching excitation. *J. Sound Vib.* **331** (13), 3199–3212.

UTSUMI, M. 2011 Theoretical determination of modal damping ratio of sloshing using a variational method. *J. Pressure Vessel Technol.* **133**, 011301-1.

ZAKHAROV, V. E. 1968 Stability of periodic waves of finite amplitude on the surface of a deep fluid. *J. Appl. Mech. Tech. Phys.* **2**, 190–194.

https://doi.org/10.1017/jfm.2012.635 Published online by Cambridge University Press